UNDERSTANDING THE ROLE OF CLIMATE AND SOCIOECONOMIC FACTORS IN DRIVING IRRIGATED AGRICULTURE DYNAMICS IN THE LOWER COLORADO RIVER BASIN

by

Cynthia L. Norton

A Thesis Submitted to the Faculty of the

SCHOOL OF NATURAL RESOURCES AND THE ENVIRONMENT

In Partial Fulfillment of the Requirements

For the Degree of

MASTER OF SCIENCE
WITH A MAJOR IN NATURAL RESOURCES

In the Graduate College

THE UNIVERSITY OF ARIZONA

2019

THE UNIVERSITY OF ARIZONA
GRADUATE COLLEGE

As members of the Master's Committee, we certify that we have read the thesis prepared by ***Cynthia Norton***, titled ***Understanding the Role of Climate and Socioeconomic Factors in Driving Irrigated Agriculture Dynamics in the Lower Colorado River Basin*** and recommend that it be accepted as fulfilling the thesis requirement for the Master's Degree.

William Kolby Smith Date: (5/3/2019)

Cynthia Wallace Date: (5/3/2019)

Willem J.D. van Leeuwen Date: (5-3-2019)

Final approval and acceptance of this thesis is contingent upon the candidate's submission of the final copies of the thesis to the Graduate College.

I hereby certify that I have read this thesis prepared under my direction and recommend that it be accepted as fulfilling the Master's requirement.

Date: (5/3/2019)

William Kolby Smith
Assistant Professor
School of Natural Resources and the Environment

ACKNOWLEDGEMENTS

I would like to thank my graduate advisor Dr. William Kolby Smith for guiding me throughout the graduate program. My sincere gratitude to committee members Dr. Cynthia Wallace and Dr. Wim van Leeuwen who warmly accepted to be on my committee and provided me with insightful suggestions and guidance. I would like to thank Dr. Matthew Dannenberg, Dr. Dong Yan, Jesus Rodriguez, Nathaniel Paul Robinson, Pratima K C, Xian Wang and Amy Hudson for helping me throughout different stages of this research and providing fundamental support for a successful research study. Finally, I would like to thank my family and friends for their advice, support, guidance, encouragement, and the patience throughout my graduate career.

TABLE OF CONTENTS

LIST OF TABLES

LIST OF FIGURES

season temperature. Despite differences in water rights, both regions correlate to dominant regional climate predictor.

Figure 8. Trends in NDVI versus climate variable for years with a split of high and low market value years. a) LCRP area linear regression of mean winter growing season NDVI versus cool season temperature with a market value split. b) PMAMA area linear regression of mean summer growing season NDVI versus warm season precipitation with a market value split. Both regions show higher biophysical signal values on high market value years compared to low market value years. This suggests a change in management practice to maximize crop productivity.

SUPPLEMENTARY FIGURES

Figure 1. Figure shows scenes path row outline overlaid on the lower Colorado Basin. Green stars show exact scene path rows chosen for regions of interest within the lower Colorado Basin.

Figure 2. Regional climate and biophysical trends within study area. a) Biophysical greenness NDVI trends for both LCRP and PMAMA b) LCRP mean growing season temperature (b) trends for all 17 years and PMAMA overall growing season precipitation trends for all 17 years. c) Market value of agricultural crop production sold trends using Arizona agricultural statistics.

Figure 3. Integrated fallowing trends for both LCRP and PMAMA regions. Image shows percent area with active crop for all 17 years. Plot shows LCRP region having overall active crop extent higher throughout all the years compared to PMAMA. Additionally, LCRP show less inter-annual variability in crop extent compared to PMAMA

Figure 4. Spatial explicit fallowing trends within both regions. Additionally, figure shows how many pixel data layers were used for spatial explicit correlations of biophysical NDVI values with climate. The brown pixels represent 15-17 years of active crop (1-2 years of fallowing) occurred in the pixel's footprint and the change in colors, fallowing years = yellow (2-4 years), green (4-6 years) and purple (6-8 years), represent additional years of fallowing has occurred. a) LCRP region spatial explicit fallowing dynamics. b) PMAMA region spatial explicit fallowing dynamics. LCRP region has less inter-annul variability in fallowing dynamics compared to PMAMA.

Figure 5: NDVI anomalies for both regions for all 17 years. Each scene shows positive or negative anomalies for both regions. The zoomed insets show spatial explicit anomalies for LCRP and PMAMA for the year 2017. The blue colors represent a positive anomaly (higher NDVI values compared to historical mean) and the red colors are negative anomalies (lower NDVI values compared to historical mean).

Figure 6: Image shows mean trends in biophysical greenness values when calculated including fallowed pixels (orange) and values without fallowed pixels (blue). The biophysical signal of crops decreased when fallowed pixels are used for calculating integrated greenness NDVI values of active crop.

ABSTRACT

Understanding the dynamics of agriculture in relation to climate and socioeconomic variables such as market value is essential in assessing water use within a semi-arid basin. This study aims to improve understanding of the spatial and temporal variability of agriculture fallowing and crop productivity using satellite Normalized Difference Vegetation Index (NDVI), meteorological observations and socioeconomic data across two regions in Arizona: the Lower Colorado River Planning (LCRP) region in LCRP County and the Active Management Areas (PMAMA) in Maricopa County and Pinal County. A key difference between these regions is there access to water for irrigation: LCRP has 1st priority (senior) irrigation water access rights, whereas PMAMA has 3rd priority (junior) irrigation water access rights. Using Google Earth Engine, I produced annual extent of fallow and active croplands at high spatial resolution (30-m) from 2001-2017 by applying the Fallow-land Algorithm based on Neighborhood and Temporal Anomalies (FANTA) driven by 8-day normalized difference vegetation index (NDVI) for each region of interest. I then evaluated how factors including weather and market value have influenced management decisions for seasonal fallowing using statistical modeling. Results show that LCRP (with senior water rights) varied very little in agricultural extent from year to year (87 - 90% active) compared to PMAMA (77 - 84% active) potentially due to regional differences in growing season and water rights. Agricultural extent and productivity in both regions was found to be sensitive to biophysical factors, with LCRP most sensitive to aridity (R^2=0.486) and PMAMA most sensitive to precipitation (R^2=0.358). Finally, we found market value significantly increased regional climate sensitivity, such that agricultural productivity was highest when both biophysical constraints were low and market values were high. This research effort provides a framework and demonstrates the importance of separately analyzing patterns of agricultural extent and productivity, which I found to interact in complex ways with both biophysical (e.g., drought) and socioeconomic (e.g., market value) factors to explain year to year variability in total regional agricultural production.

INTRODUCTION

Irrigated agriculture accounts for 40% of global crop production, which contributes to food and feed production within semi-arid and arid regions (Chen et al. 2018). Globally, between 70 to 80% of fresh water is used for irrigation, which puts pressure on the water supply especially as food demand continues to increase in congruence with population increase (Bastiaanssen et al. 2000). Additionally, water use is expected to increase as evapotranspiration rates increase due to a warmer planet, rising vapor pressure deficit and intensifying droughts (Shivers et al., 2019; Bates et al. 2008). Climate variability, crop prices, water policies, crop rotation and the dynamics of fallowed agriculture all drive irrigated cropland interannual variability (Deines et al. 2017; Brown & Pervez, 2014; Ozdogan & Gutman, 2008; Wisser et al., 2008). Additionally, drought continues to create shortages on water supply in the western United States. Sustainable water management is necessary to mitigate the impacts of population growth and increasing food demands on water resources.

The Colorado River Basin encompasses seven states and provides municipal and industrial water to millions of people across all major southwestern cities both inside and outside the basin. Irrigation accounts for about 70% of water demand within the basin, which exists in an arid climate where precipitation is relatively low (average 250mm/year). Within the lower Colorado River basin, differences in crop intensity are observed due to climate conditions, water table, irrigation water availability, farmer management and market conditions (Fan et al. 2014).
It is anticipated that the changing climate will affect crop yields and regional agriculture patterns partly as management decides to change crop type or fallow fields (Shivers et al 2018). Crop

management decisions impact communities in ways through economic variables, food security and regional water availability (Wallace et al. 2017, Shivers et al 2018). One important metric for measuring agriculture water use is through the amount of irrigated area that is left unplanted or fallow (Wallace et al. 2017). Therefore, monitoring crop changes, such as fallowing, are necessary in assisting long-term planning for managers, policymakers, scientists and farmers. Producing accurate, timely maps of fallowed and active crop extent is a critical factor needed to better understand agriculture water use and food supply (Wallace et al. 2017).

Spatially explicit data sets that accurately map growing season fallowing dynamics would provide: 1) insight into variables that influence irrigation dynamics; 2) improved understanding of climate effects on agriculture value; and 3) decision support for land managers regarding growing season water budgets (Deines et al. 2017). Researchers have used remotely sensed data as a recognized framework for creating land use and land cover classifications and have the potential for mapping and monitoring crop changes with more efficiency compared to the intense labor of ground mapping (Anderson 1976, Galvão et al. 2018). For instance, a paper published by Gumma et al. 2018 used Moderate Resolution Imaging Spectroradiometer (MODIS) satellite images to identify cropland fallows and active areas in Mynmar for one year of growing season. They found annual cropland fallowing variability that ranged from 56.5% to 82.7%. A case study in western Niger done by Ton et al. 2017 quantify cropland active and fallowed areas using a fuzzy classifier. They found a decrease in NDVI over a 14-year time period with an increase in crop field area. Another study done in 2018 by Chen and collaborations used remote sensing greenness index to assess irrigation events for part of a growing season in the Hexi Corridor of northwestern China and found an overall accuracy of 87%. These past research studies on

irrigation dynamics, however, have used relatively low-resolution datasets and have typically overlooked the relationship between climate variables (e.g. vapor pressure deficit, precipitation, temperature) and management decisions such as fallowing, with some exceptions from Wallace et al. 2017, Deines et al 2017 and Chance et al 2017. This study builds from the research done in the Wallace et al. 2017 paper, Deines et al. 2017 paper and Chance et al. 2017. Researchers in the Wallace paper created 17 years of annual maps of active and fallowed crop in Central Valley California while Deines et al. 2017 and Chance et al. 2017 created high resolution annual extent maps from 1999-2016 and assessed irrigation dynamics over time with climate and a socioeconomic variable. As shown in these past research efforts, annual spatially explicit data sets capture differences in irrigation dynamics that static maps or non-spatial datasets cannot capture well, thus providing a novel perspective and opportunity for insights into the factors driving dynamics of agricultural landscapes.

The research presented here aimed to estimate and evaluate the extent of fallow and active croplands seasonally at high spatial resolution (30-m) from 2001-2017 by applying the Fallow-land Algorithm based on Neighborhood and Temporal Anomalies (FANTA) driven by 8-day normalized difference vegetation index (NDVI) data (Wallace et al., 2016 and Wallace in prep). FANTA is run through the Google Earth Engine (GEE) interface using a program written by Jesus Rodriguez (USGS postdoc); it was developed for the Central Valley of California using 8-day MODIS NDVI composites (Wallace et al., 2016) and was modified for a separate study (Byrd et al., 2019) to use Landsat-scale NDVI composite data (Wallace et al., in prep). The GEE program producing Landsat-scale FANTA maps developed by the USGS was made available for this project. For this project, Landsat-based FANTA was run in GEE specifying the study area in

Arizona and accessing all available Landsat and MODIS images from January 1, 2001 to December 31, 2017, producing a binary map for each year the depicts planted (active) versus fallowed cropland.

A second source of NDVI data were accessed for this study, namely the active cropland growing season integrated NDVI (iNDVI) produced by Robinson et al. 2017. iNDVI is a 16-day composite dataset derived from Landsat images that uses a climatology approach to fill missing data; it was also accessed through GEE.

Finally, the relationships between both the active crop extent dynamics derived from FANTA and the growing season crop productivity derived from iNDVI with key biophysical and socioeconomic factors were explored. Biophysical factors included warm and cool season temperature, precipitation, and aridity, whereas socioeconomic factors included water rights and market value. The main goal of this work was to develop a framework for improved agriculture monitoring and decision-making and enable new understanding of the importance of biophysical and socioeconomic factors in mediating agriculture production dynamics within the Colorado River Basin.

I. Goals and objectives

The main objective of this study is to examining the spatiotemporal dynamics of agriculture management and vegetation response to climate and socioeconomic incentives within a semi-arid region with depleting water sources. The study takes advantage of remote sensing imagery through Google Earth Engine (GEE) as an opportunity to assess agriculture biophysical and management response to climate. The main research questions are as follows:

1) What are the annual trends of agricultural fallowing within two regions in the Colorado River Basin during a 17-year period (2001 – 2017)?
2) How do dominant growing season active crop extent and productivity within these regions respond to precipitation, temperature, vapor pressure deficit and aridity?
3) How do socioeconomic factors such as water rights and market value of agriculture production influence cropland extent and productivity dynamics?

I examine the relationships between socio-economics, agriculture dynamics and climate variables by: (1) creating annual maps of active and fallow using the FANTA algorithm; (2) determining the dominant climate predictor for crop NDVI and % active extent dynamics; and (3) assessing how agricultural market value strengthen or weaken statistically significant climate predictors and their relationships with active crop dynamics. My main objective is to create a reliable methodology through the GEE interface to enable new understanding of the importance of biophysical and socioeconomic factors in mediating agriculture production dynamics within the Colorado River Basin.

PRESENT STUDY

The methods, results, and conclusions of this study are presented in the paper appended to this thesis. The following is a summary of the most important findings in this document.

I. Summary

The primary aim of this study is to develop annual agriculture fallowing maps to understand and explore active crop dynamics and associated drivers within an arid region. The study takes advantage of remote sensing imagery through GEE as an opportunity to assess agriculture biophysical and management response to climate. A novel methodology was applied to remote sensing satellite imagery over two regions within the lower Colorado River Basin: Lower Colorado River planning (LCRP) and southcentral Arizona Pinal and PMAMA Active Management Area (PMAMA). Annual maps of fallowed and active croplands were created at 30-m spatial resolution from 2001-2017 by applying the Fallow-land Algorithm based on Neighborhood and Temporal Anomalies (FANTA) (Wallace et al., 2016). FANTA was developed for the Central Valley of California using 8-day MODIS NDVI composites (Wallace et al., 2016) and was modified for a separate study (Byrd et al., 2019) to use Landsat-scale NDVI composite data (Wallace et al., in prep). The GEE program producing Landsat-based FANTA maps was made available for this project through the USGS. For this project, Landsat-based FANTA was run in GEE specifying the study area in Arizona and accessing all available Landsat and MODIS images from January 1, 2001 to December 31, 2017, producing a binary map for each year that depicts planted (active) versus fallowed cropland.

I then evaluated the spatio-temporal relationship between cropland extent and productivity and biophysical factors including temperature, precipitation, vapor pressure deficit (VPD), aridity derived from the Parameter Regression on Independent Slopes Model (PRISM) meteorological dataset. Linear regression statistical models were used to quantify and significant correlation

and/or sensitivity of active crop dynamics to seasonal climate predictors as well as yearly agriculture market value variations.

II. Conclusions

The main objective of this research was to assess agricultural fallowing dynamics and crop productivity within the Lower Colorado River Basin. The FANTA model results were validated using ground observations that are collected in some years by the USGS and made available for this study. Validation results for 2014 showed that FANTA had an overall accuracy of 95% and 88% on PMAMA and LCRP, with active and fallow user's accuracy of 99% and 71% for the PMAMA and 96% and 82% for the LRCP with producer's accuracy of 95% and 93% for the PMAMA and 77% and 98% for the LRCP I next evaluated trends in cropland extent and productivity and their relationship with key biophysical and socioeconomic factors as described above for each region I found that LCRP (senior water rights) varied very little in agricultural extent from year to year (87-90% active) compared to PMAMA (77-84% active) potentially due to regional differences in growing season and water rights. Agricultural extent and productivity in both regions was found to be sensitive to biophysical factors, with LCRP most sensitive to aridity (R^2=XX) and PMAMA most sensitive to precipitation (R^2=0.351). Finally, I found market value increased regional climate sensitivity, such that agricultural productivity was highest when both biophysical constraints were low and market values were high. The framework I have developed utilizes simple freely available, near real-time data inputs to produce information of high value to regional scientist and land managers. The framework enables the separation of fundamental land management decisions such as the decision to crop a given land parcel as well as the decision to allocate resources to a given land parcel. The separation of these key factors further enables the exploration of their correlation to biophysical factors such as drought and socioeconomic factors such as the value of the crop. Additionally,

the approach that I have developed is transferable to other regions by simply updating the input data and tuning a few key parameters related to seasonal growing season timing. These new data of agricultural extent and production provide critical information for land managers, modelers and decision makers.

III. Future Work

This study could be further enhanced by 1) the consideration of crop types and 2) consideration of irrigation district boundary. Additionally, the relationship between vegetation productivity and climate patterns could be further explored by incorporating other datasets such as water sources, irrigation type and lag responses.

Considering irrigation district boundary can help in understanding trends within different irrigation districts and how the difference in district water use influence crop dynamics within the area. Looking at the differences in district water use will give us insight on the spatial variability of fallowing dynamics and active crop relationships with climate and socioeconomic variables. Irrigation district boundaries can be acquired through the Arizona Department of Water Resources GIS data. Additionally, on-the-ground agricultural practices such as predominant crop type, can result in different NDVI values over time. Considering crop types could aid in minimizing classification errors and give us insight on the drivers of greenness values and extent changes. This dataset can be found using the CropScape – NASS CDL Program (https://nassgeodata.gmu.edu/). CropScrape produces cropland raster data layer with crop-specific land cover map.

REFERENCES

Anderson, J. R. (1976). A land use and land cover classification system for use with remote sensor data (Vol. 964). US Government Printing Office.

Bastiaanssen, W. G., Molden, D. J., & Makin, I. W. (2000). Remote sensing for irrigated agriculture: examples from research and possible applications. Agricultural water management, 46(2), 137-155.

Bontkes, T. S., & van Keulen, H. (2003). Modelling the dynamics of agricultural development at farm and regional level. Agricultural Systems, 76(1), 379-396.

California Department of Food and Agriculture. California Agricultural Statistics Review 2014–2015. Available online: https://www.cdfa.ca.gov/statistics/PDFs/2015Report.pdf (accessed on 10 July 2018).

Challinor, A.J.; Watson, J.; Lobell, D.B.; Howden, S.M.; Smith, D.R.; Chhetri, N. A meta-analysis of crop yield under climate change and adaptation. Nat. Clim. Chang. 2014, 4, 287–291.

Chance, E., Cobourn, K., & Thomas, V. (2018). Trend detection for the extent of irrigated agriculture in Idaho's Snake river plain, 1984–2016. Remote Sensing, 10(1), 145.

Chen, Y., Lu, D., Luo, L., Pokhrel, Y., Deb, K., Huang, J., & Ran, Y. (2018). Detecting irrigation extent, frequency, and timing in a heterogeneous arid agricultural region using MODIS time series, Landsat imagery, and ancillary data. Remote Sensing of Environment, 204, 197-211.

Cohen, M. J., Martin, J. C., Ross, N., & Luu, P. (2011). Municipal Deliveries of Colorado River Basin Water. Pacific Institute, Berkeley, California, USA.

Deines, J. M., Kendall, A. D., & Hyndman, D. W. (2017). Annual irrigation dynamics in the US northern high plains derived from Landsat satellite data. Geophysical Research Letters, 44(18), 9350-9360.

Galletti, C. S., & Myint, S. W. (2014). Land-use mapping in a mixed urban-agricultural arid landscape using object-based image analysis: A case study from Maricopa, Arizona. Remote Sensing, 6(7), 6089-6110.

Galvão, L. S., Epiphanio, J. C. N., Breunig, F. M., & Formaggio, A. R. (2018). 6 Crop Type Discrimination Using Hyperspectral Data. Biophysical and Biochemical Characterization and Plant Species Studies, 183.

Gianelli, W. R. 2015. Water Leaders 2015 Class Report: Managing Drought for the Economy and the Environment. Sacramento, CA: Water Education Foundation. http://www.watereducation.org/post/2015-class-report.

Gumma, M. K., Thenkabail, P. S., Deevi, K. C., Mohammed, I. A., Teluguntla, P., Oliphant, A., ... & Whitbread, A. M. (2018). Mapping cropland fallow areas in myanmar to scale up sustainable intensification of pulse crops in the farming system. GIScience & remote sensing, 55(6), 926-949.

Nuckols, J.R.; Gunier, R.B.; Riggs, P.; Miller, R.; Reynolds, P.; Ward, M.H. Linkage of the California Pesticide Use Reporting Database with spatial land use data for exposure assessment. Environ. Health Perspect. 2007, 115, 684.

Tong, X., Brandt, M., Hiernaux, P., Herrmann, S. M., Tian, F., Prishchepov, A. V., & Fensholt, R. (2017). Revisiting the coupling between NDVI trends and cropland changes in the Sahel drylands: A case study in western Niger. Remote sensing of environment, 191, 286-296.

Wallace, C. S., Thenkabail, P., Rodriguez, J. R., & Brown, M. K. (2017). Fallow-land Algorithm based on Neighborhood and Temporal Anomalies (FANTA) to map planted versus fallowed croplands using MODIS data to assist in drought studies leading to water and food security assessments. GIScience & Remote Sensing, 54(2), 258-282.

Wu, Z., Thenkabail, P. S., Mueller, R., Zakzeski, A., Melton, F., Johnson, L., ... & Verdin, J. P. (2014). Seasonal cultivated and fallow cropland mapping using MODIS-based automated cropland classification algorithm. Journal of Applied Remote Sensing, 8(1), 083685.

Shivers, S., Roberts, D., McFadden, J., & Tague, C. (2018). Using Imaging Spectrometry to Study Changes in Crop Area in California's Central Valley during Drought. Remote Sensing, 10(10), 1556.

APPENDIX A:

UNDERSTANDING THE ROLE OF CLIMATE AND SOCIOECONOMIC FACTORS IN DRIVING IRRIGATED AGRICULTURE DYNAMICS IN THE LOWER COLORADO RIVER BASIN

To be submitted to "Environmental Research Letters"

Cynthia Norton [1*], Matt Dannenberg[1], Cynthia Wallace[2], Jesus Rodriguez[3] and William Smith [1]

[1] School of Natural Resources and the Environment, University of Arizona, 1064 East Lowell Street Tucson, AZ 85721, USA

[2] Western Geographic Science Center, U.S. Geological Survey, Tucson, AZ 85719, USA

[3] Western Geographic Science Center, U.S. Geological Survey, Tucson, AZ 85719, USA

E-mail *: cnorton1@email.arizona.edu

ABSTRACT

The Colorado River Basin encompasses seven states and provides municipal and industrial water to millions of people across all major southwestern cities both inside and outside the basin. Irrigation accounts for about 70% of water demand within the basin since it exists in an arid climate where precipitation is relatively low (average 250mm/year). Past research on irrigation dynamics has generally utilized relatively low-resolution datasets and has typically overlooked the relationship between climate and management decisions such as fallowing. In this study, annual extent of fallow and active croplands were mapped at high spatial resolution (30-m) from 2001-2017 by applying the Fallow-land Algorithm based on Neighborhood and Temporal Anomalies (FANTA) in the Google Earth Engine (GEE) computing environment driven by 8-day normalized difference vegetation index (NDVI) data derived from Landsat and Moderate-resolution Imaging Spectroradiometer (MODIS) satellite images (Wallace et al., 2016). Growing season crop productivity within active agriculture was estimated using 8-day composite iNDVI data produced by Deines et al. 2017 and accessed in GEE. Relationships between both annual cropland extents derived from FANTA and crop productivity derived from iNDVI with various factors including water rights, market value and climate variables were explored. Results show that the Lower Colorado River Planning (LCRP) region in LCRP County varied very little in agricultural extent from year to year, with 87-90% of croplands active, compared to the PMAMA-Maricopa Active Management Area (PMAMA), with 77-84% croplands active. This difference is likely due to regional differences in growing season and water rights, with LCRP possessing senior water rights and reliably warmer winters and PMAMA possessing junior water rights with more variable winter temperatures. Agricultural extent and productivity in both regions was found to be sensitive to biophysical factors, with LCRP most sensitive to aridity (R^2=0.486) and PMAMA most sensitive to precipitation (R^2=0.351). Finally, market value was found to increase regional climate sensitivity, such that agricultural productivity was highest when both biophysical constraints were low and market values were high. This suggests that high market values increased productivity based on demand and climate drivers as agricultural managers invest more resources on increasing productivity. Our findings help explain how biophysical (e.g., drought) and socioeconomic (e.g., market value) factors interact to produce annual patterns in cropland extent, productivty and water use, potentially informing regional climate adaptation strategies.

Keywords: fallow, remote sensing, NDVI

1. INTRODUCTION

Irrigated agriculture currently accounts for roughly 40% of global cropland production and nearly 70% of global fresh water demand, which highlights the critical linkage between global food security and freshwater availability. Current research indicates that freshwater availability will become more stressed in the future due to: 1) increasing food demand as population increases and diets shift (Bastiaanssen et al. 2000); and 2) freshwater availability decreases due to rising atmospheric aridity and intensifying drought severity and frequency (Shivers et al., 2019; Bates et al. 2008). In particular, the Colorado River basin provides a majority of the water demands within seven states U.S. states and 34 Native American tribes (Pulwarty et al. 2005). Water flow in Colorado River Basin is known to be one of the highest legislated and managed basins in the world with large scale withdrawals and impoundments (Pulwarty et al. 2005). In the semiarid lower Colorado River Basin, small scale changes in precipitation can have large scale impacts on water supplies (Pulwarty et al. 2005). Conflicts regarding water allocation and water rights have played out as variability in climate affect water availability, increasing demands, water quality and ground water depletion effects the dynamics of water within the basin (Pulwarty et al. 2005). Management within the Colorado River Basin have been exposed to many transboundary interactions through negotiations and litigation as society decides on water allocation under a changing climate (Pulwarty et al. 2005). Additionally, a study has shown that 99% of water use for energy or food within the Lower Colorado Basin goes to the production of agriculture (Huckleberry et al. 2019). Therefore, monitoring dynamics, such as fallowing, are necessary in assisting long-term planning for managers, policymakers, scientists and farmers. The Colorado River Basin encompass socio-economic and environmental complexities that

increase the need to for datasets to understand and optimize how our limited water resources are utilized across these water limited regions. Producing accurate, timely maps of fallowed and active crop extent is a critical factor needed to better understand agriculture water use and food supply (Wallace et al. 2017).

Changes in biophysical constraints such as drought frequency could affect crop production by either changing cropland extent (i.e., the total area in planted in a given year) or agricultural productivity (i.e., the average production or crop yield on a given parcel of active cropland) as well as influence regional agriculture patterns as management decides to change crop type or fallow fields (Shivers et al 2018). Thus, an important metric for better understanding regional agriculture production strategies is through quantification of the amount of irrigated area that is left unplanted or fallowed (Wallace et al. 2017). Producing accurate, timely maps of fallowed and active crop extent is a critical step towards improved understanding of agriculture production and water use (Wallace et al. 2017). Spatially explicit data sets that accurately map growing season fallowing dynamics provide: 1) insight into variables that influence irrigation dynamics; 2) improved understanding of climate effects on agriculture value; and 3) decision support for land managers regarding growing season water budgets (Deines et al. 2017).

Remotely sensed data have been used to create land use and land cover classifications with more efficiency when compared to the intense labor of ground mapping (Anderson 1976, Galvão et al. 2018). These data are also used to map and monitor crop dynamics. For example, Gumma et al. 2018 used Moderate Resolution Imaging Spectroradiometer (MODIS) satellite images to identify cropland fallows and active areas in Mynmar for one year of growing season. They found annual

cropland fallowing variability that ranged from 56.5% to 82.7% in various districts across the country. A case study in western Niger done by Ton et al. 2017 quantify cropland productivity as well as extent of active and fallowed areas using a fuzzy classifier. They found a decrease in NDVI over a 14-year time period with an increase in crop field area. Another study done in 2018 by Chen and collaborations used remote sensing greenness index to assess irrigation events for part of a growing season in the Hexi Corridor of northwestern China and found an overall accuracy of 87%. These past research efforts on irrigation dynamics, however, have generally utilized relatively spatially-coarse datasets and have typically not explored relationships between climate variables (e.g. vapor pressure deficit, precipitation, temperature, etc.) and management decisions affecting cropland dynamics and pattern, with some exceptions from Wallace et al. 2017 and Deines et al 2017. This study builds on the research of Wallace et al. 2017 and Deines et al. 2017. Researchers in the Wallace paper created 17 years of annual maps of active and fallowed crop in Central Valley California while Deines et al. 2017 created high resolution annual extent maps from 1999-2016 and assessed irrigation dynamics over time. In comparing t past research, their results in overall trend, drivers and variances, show that these early efforts suggest that annual spatially explicit data sets present a novel perspective on the differences in irrigation dynamics that static maps or non-spatial datasets cannot capture well.

This research aims to estimate and evaluate the extent of fallow and active croplands annually at high spatial resolution (30-m) from 2001-2017 by applying the Fallow-land Algorithm based on Neighborhood and Temporal Anomalies (FANTA) driven by 8-day normalized difference vegetation index (NDVI) data (Wallace et al., 2016). Additionally, active cropland growing-season integrated NDVI (iNDVI) and extent dynamics were explored by evaluating their

relationship to key biophysical and socioeconomic factors. Through Google Earth Engine (GEE) interface and using a U.S. Geological Survey (USGS) program made available for this study, all available Landsat and MODIS product were accessed from January 1, 2001 to December 31, 2017 to create annual binary maps of planted versus fallowed cropland. iNDVI was also accessed through GEE as a 16-day composite dataset derived from Landsat images that used a climatology approach to fill missing data. Biophysical factors considered included warm and cool season temperature, precipitation, and aridity, whereas socioeconomic factors included water rights and market value. The main goal of this work was to develop a framework for improved agriculture monitoring and decision-making and enable new understanding of the importance of biophysical and socioeconomic factors in mediating agriculture production dynamics within the Colorado River Basin.

2. METHODS

2.1 Study Area

The study area consists of two different areas within the lower Colorado River Basin. The basin provides water to roughly 35 million people within and outside the water shed such as Las Vegas, Tucson, LCRP, PMAMA, Denver and Los Angeles (Cohen et al. 2011). The study specifically focuses on south-western Arizona agriculture within Lower Colorado River planning (LCRP) in LCRP County and southcentral Arizona Pinal and Maricopa County Active Management Areas (PMAMA). Both study areas consist of agriculture fields that are large suppliers of lettuce, alfalfa, cotton, cauliflower and broccoli (Acker et al. 2010). Southwestern Arizona agriculture is primarily within LCRP. LCRP is characterized as a hot arid desert and is known as the sunniest city and the lettuce capital of the country - producing 90% of the leafy vegetables within the United States (14, 15). The overall warm, dry climate within LCRP and access to water from the Colorado River basin makes for a thriving agricultural business. While

PMAMA is characterized as a hot desert steppe. The biggest difference between areas is that the amount of precipitation is far less within LCRP compared to the other counties (Smith 1956). Another distinguishing characterization between the agriculture areas is the source of irrigation water and water rights. PMAMA has junior water rights and gets irrigation water from ground water, effluent and the Central Arizona Project (CAP), which diverts water from the Colorado River and transferred hundreds of miles to the districts. In contrast, LCRP has senior water rights and gets irrigation water directly from the surface water diverted from the Colorado River and some ground water. The difference between water rights is a major factor. LCRP has some of the oldest water rights on the river that gives them 1st priority (senior) in accessing water from the basin. On the other hand, PMAMA has 3rd priority rights (junior) to surface water which means that they have limited access to water during drought years. As a note, 2nd priority water rights are….

Figure 1. Figure shows scenes path row outline overlaid on the lower Colorado Basin. Green stars show exact scene path rows chosen for regions of interest within the lower Colorado Basin

2.2 Satellite Imagery, Vegetation Indices, Meteorological Data and Economic Variable

For the FANTA classification, both Landsat and MODIS data were used and accessed through GEE and included all data available from January 1, 2001 to December 31, 2017. Landsat imagery is collected every 16 days at 30-m resolution and includes reflectance bands from visible through near-infrared and into shortwave infrared; each image is approximately 175 x 185 km and 6 scenes are required to cover the study area. Between 2001 and 2017, data from Landsat satellites 5, 7 and 8 are available, such that overlapping missions result in up to 4 scenes per month. MODIS imagery is collected daily at a 250-m resolution. We accessed MODIS 8-

day Normalized Difference Vegetation Index (NDVI) data. The NDVI is a measure of photosynthetically active vegetation (reference) and is calculated as follows:

$$NDVI = \frac{(NIR - RED)}{(NIR + RED)}$$

where NIR is near infrared reflectance and RED is visible red reflectance. The MODIS 8-day NDVI composite is produced by selecting the pixel obtained during the 8-day period that contains the best possible observation as evaluated on the basis of favorable coverage and view angle, the absence of cloud contamination, and aerosol loading (http://modis-sr.ltdri.org/products/MOD09 UserGuide_v1_3.pdf), resulting in a relatively cloud-free image using data that are pre-filtered for quality.

To quantify annual growing-season crop productivity, we accessed a calibrated and processed iNDVI product through GEE. These data (Robinson et al. 2017) were corrected for cloud cover and processed so that scene edge differences were smoothed and missing values were filled using historical climatology data. The iNDVI data were provided on a 16-day time step from 2001 to 2017. Meteorological data, market value and the USGS National Land Cover Database (NLCD) were compiled for statistical analyses and far masking agriculture outer extent (Text S1). PRISM meteorological data was provided on a monthly time step from 2001 to 2017. Each year was then divided into seasons:

Table 1: Seasonal divisions of research variables such as NDVI and meteorological data.

2.3 Mapping Agricultural Fallowing and Extent

Annual maps of fallowed and active croplands were created at 30-m spatial resolution from 2001-2017 by applying the Fallow-land Algorithm based on Neighborhood and Temporal

Anomalies (FANTA) (Wallace et al., 2016). FANTA was developed for the Central Valley of California using 8-day MODIS NDVI composites (Wallace et al., 2016) and was modified for a separate study (Byrd et al., 2019) to use Landsat-scale NDVI composite data (Wallace et al., in prep). The GEE program producing Landsat-based FANTA maps was made available for this project through the USGS. For this project, Landsat-based FANTA was run in GEE specifying the study area in Arizona and accessing all available Landsat and MODIS images from January 1, 2001 to December 31, 2017, producing a binary map for each year that depicts planted (active) versus fallowed cropland. The FANTA examines each pixel and compares its status (monthly maximum greenness and monthly dynamic range in greenness) to its historical condition and to the status of other cultivated pixels in its climate division (i.e., neighborhood). As written for the Central Valley of California, the algorithm evaluates both an "early" and "normal" growing season by considering April-May and June-July, respectively. We examined growing season calendars for both LCRP and PMAMA and determined that these 4 months overlap the growing seasons in our areas and, therefore, we applied FANTA without adjusting the months evaluated (Figure 4).

The Landsat composites used in FANTA were created in GEE by accessing all Landsat images within each 8-day MODIS composite interval, masking clouds and shadows, calculating NDVI, and selecting the maximum NDVI for the 8-day interval – producing up to four values for each month. Monthly NDVI maximum and minimum values needed for the FANTA algorithm were then produced by first looking (for each year) for the month with the fewest no-data pixels, typically May or June. Any gaps for this month were then filled using MODIS data weighted by the Landsat:MODIS NDVI relationships observed in the temporally adjacent images at that pixel (Wallace et al., in prep). If both the month prior and the month after the missing value in the

"best" month have valid pixels, the relationship is averaged; otherwise the single relationship is used to weight the MODIS value (Wallace et al., in prep). This results in one image that is complete for the year. Gaps in the remaining months for the year are filled outward from this complete month by again weighting the MODIS NDVI value with the observed Landsat:MODIS NDVI relationship in the temporally-adjacent image. The monthly maximum and minimum values are then subtracted to produce the monthly range value needed for FANTA.

The binary map of FANTA asks four questions (Wallace et al., 2016):

1. Does the pixel LOOK like a crop based on its history?
2. Does the pixel ACT like a crop based on its history?
3. Does the pixel LOOK like a crop compared to its neighbors?
4. Does the pixel ACT like a crop compared to its neighbors?

If the answer to any 2 of these questions is "No", the pixel is mapped as fallowed.

Extracting overall cropland extent and omitting fallow lands was done by masking classified layers with the NLCD classified agriculture (81). This gives agricultural extent a boundary layer for extracting active cropland pixels. Validating the models was done by a producing a point data set within ArcMap Esri4.

Validation were done using arcgis to create 100 random points within each polygon, extracted FANTA values to those points and then spatially joined validation values with classification values. The attribute table was used to create a confusion matrix to assess producer, user and overall accuracy. Validation polygons such as u of a facilities were removed from validation

points. PMAMA validation included two crop rotations while LCRP had four. Fallow and abandoned was considered as fallow while all crop types were active for both areas. For active validations, active crop was accurately classified if any of the validation rotations had active crop. Active was mistakenly classified as fallow if all validated rotations were fallow. Fallow validations with all active crop rotations was incorrectly classified as fallow while instances with fallowing rotations was considered accurately classified.

Figure 2. Figure shows an example of the methodology for masking. Masking starts from masking the biophysical signal true color composite (a and d) with the orange colored symbolized NLCD (b and e) and then masking with the FANTA classified map, symbolized with blue. The orange colors peeking out of the blue agriculture active crop extent show areas in fallow during the growing season of the year. a) LCRP County southwest Arizona true color image. b) LCRP County southwest Arizona NLCD overlay. c) LCRP County southwest Arizona FANTA overlay. d) South central PMAMA Arizona area true color image. e) South central PMAMA Arizona area NLCD f) South central PMAMA Arizona area FANTA.

2.4 Active Crop Trends

We assessed active crop trends by looking at the interannual dynamics of percent fallowing (derived from FANTA) as well as extracting iNDVI values within active cropland and exploring dynamics of crop productivity and relationships between iNDVI and biophysical/sociological variables. To extract pure active cropland for each year, the total maximum agricultural boundary extent was identified using the NLCD classification and fallowed cropland was masked using the binary FANTA classification. A time series of average iNDVI and active crop extent from 2001-20017 was extracted from all the data.

2.5 Analyzing Active Crop Correlations with Meteorological and Economic Indicators

NDVI and meteorological data was extracted for a mean or sum value during cool and warm seasons of each year (Table 1). Results of the seasonal meteorological values were correlated with NDVI growing season mean values and yearly agricultural active crop extent. Linear regressions in R-studio was used for finding the strongest correlations with meteorological data, active crop NDVI mean values and active crop extent.

Market values were calculated using prices received surveys and indexes. The National Agricultural Statistics Service (NASS) uses monthly and annual surveys to estimate prices the producers get for crop commodities to estimate the value of agricultural production. Values of production was given by multiplying price per bushel and production for each year. Overall value of crop production was done by calculating value for each crop type and added all together. Market value is directly related to supply and demand of agricultural crops, the prices market set for their product and can influence decisions at a farm level (Bontkes and van Keulen 2003). Working in anomaly space, high and low value years were categorized and used to couple the relationships between extent, NDVI, economics and climate. Linear regressions between NDVI, climate, and extent within different value years were done to assess the difference in relationships. Spatially, correlations were done by using the same division of seasonal extents of NDVI and FANTA with climate drivers.

Figure 3. Image shows flow chart of research methodology. The chart shows datasets used for masking active crop biophysical signal. Image shows which parts of the methodology corresponds to specific research question. The FANTA classification step (1) aids in assessing

inter-annual trends of agricultural fallowing and active crop extent dynamics. Within the R-studio interface, the NLCD was used to mask agricultural boundaries while FANTA was used to mask active crop and fallow biophysical NDVI signal. This leads to the creating linear models to assess biophysical active crop signal response to climate (2). The third step (3), addresses socioeconomic drivers of NDVI and its influence to the relationship between climate and NDVI.

3. RESULTS

3.1 Classification Performance

Visually, there was good agreement between AZ-FANTA, ground level validations and Landsat composites during 2017 for LCRP and 2014 for PMAMA (Figure 5). Our point test data set found an overall accuracy for PMAMA in 2014 of 84.6% while LCRP had an overall accuracy of 88.6% for 2017. The active cropland class had an error of omission value of 6.4% for PMAMA and 0% for LCRP.

Figure 5. Image shows a visualization of classification accuracy. The outlined polygons represent validation data provided by the USGS while filled colors are from the classified FANTA image. a) LCRP area 2017 ground validation polygons overlaid on FANTA for the year 2017. b) PMAMA area 2014 ground validation polygons overlaid on a 2014 FANTA layer. If the green outline is overlaid over the green classification, this resulted in an accurately classified active plot while green outline over fallow classification symbolized as brown results in an incorrectly classified plots. Red outline over brown overlaid FANTA results in an accurately classified fallow plot while red outline over green overlaid means it was a fallow plot classified as active.

3.2 Active Crop Area Trends

Different drivers such as water management, market value and annual climate variation impact farmer irrigation decisions which in turn influence spatiotemporal crop dynamics. I assessed any variability in active extent from year to year. Additionally, I investigated how these drivers interact to regulate irrigation dynamics within the study areas. Active irrigated crop within both areas showed no substantial evidence of any change in rate of fallowing within both PMAMA and LCRP.

3.3 Meteorological Determinants and Economic Variable

Correlation matrices showed that within different areas showed significant correlations between active crop different variables (Figure 6). PMAMA active crop area revealed a positive correlation with cool season aridity ($r = 0.211$, $p = 0.04$) while active crop NDVI had a positive correlation with warm season precipitation ($r = 0.351$, $p = 0.007$). On the other hand, LCRP active crop NDVI positively correlated with cool season temperature ($r = 0.486$, $p = 0.001$) and active crop extent positively correlated with cool season temperature ($r = 0.219$, $p = 0.03$).

Figure 6. Significant linear regressions on irrigated area over time, crop NDVI and associated drivers a) LCRP area linear regression of mean winter growing season NDVI versus cool season temperature b) LCRP area linear regression of percent irrigated active crop versus yearly mean temperature c) PMAMA linear regression of mean summer growing season NDVI versus warm season precipitation d) PMAMA linear regression of percent irrigated active crop versus cool season aridity (P/PET).

Figure 6. Significant linear regressions on irrigated area over time, crop NDVI and associated drivers. a) LCRP area linear regression of mean winter growing season NDVI versus cool season temperature. b) LCRP area linear regression of percent irrigated active crop versus yearly mean temperature. c) PMAMA area linear regression of mean summer growing season NDVI versus warm season precipitation d) PMAMA area linear regression of percent irrigated active crop versus cool season aridity (P/PET). LCRP region showed biophysical response signal NDVI and extent sensitivity to dominant climate predictor cool season average temperature. PMAMA biophysical signal and extent show sensitivity to precipitation and cool season aridity.

Agricultural market value produced by the United States Department of Agriculture (USDA) within the National Agricultural Statistics Service (NASS) reflect management decisions made during the growing season such increasing crop production area. NASS utilized commodity price estimates for crop value by using prices received from various monthly surveys conducted to estimate market value. Market value, the amount of which something can be sold in a given market, reflects the fluctuations within crop supply and demand. Correlation matrices analyzing both study areas show that during high demand years, LCRP and PMAMA significantly correlated NDVI and climate predictor ($r = 0.638$, $p = 0.004$ and $r = 0.539$, $p=0.008$).

Figure 8. Trends in NDVI versus climate variable for years with high and low market values a) LCRP area linear regression of mean winter growing season NDVI versus cool season temperature b) LCRP area linear regression of percent irrigated active crop versus cool season temperature c) PMAMA linear regression of mean summer growing season NDVI versus warm season precipitation d) PMAMA linear regression of percent irrigated active crop versus warm season precipitation.

Table 2.

4. DISCUSSION

Understanding the impact of management decisions on the dynamics of agriculture productivity and fallowing is important in assessing water use within the Colorado River Basin. Additionally, parsing the relationships between active crop greenness, active crop extent, market value and their relationship with climate and greenness can give insight on how managers make decisions based on climate, economics and how this impacts crop greenness. In this study, I show that management decisions on active crop extent and greenness is influenced by the dominant climate predictor within the area and agricultural market values. New tools utilized in this research possess high spatial resolution and large amounts of imagery data which aid in overcoming the limitations of satellite imagery in mapping regional scale maps of crop dynamics. (Seifert 2018 ERL). Previous studies analysing crop, climate and management dynamics found that irrigation extent is influenced by precipitation and commodity price (Deines et al 2017). Additionally, most research that involve mapping annual irrigation dynamics tend to have low resolution, single year, statistical snapshots that do not consider crop temporal dynamics. The approach here uses a high spatiotemporal dataset to produce high resolution maps of annual active crop and fallow spatial explicit locations and links climate and economic variables to show the dynamic complexities of irrigated agriculture within the lower Colorado River Basin.

Active crop vs fallowed have high inter-annual variability during drought and non-drought years which makes mapping these dynamics important in assessing food and water security. Various approaches in assessing these dynamics typically use time-consuming collection of ground data or agricultural statistics that rely on user reports that may introduce bias. A previous study utilizing FANTA model with courser resolution MODIS satellite images

proved to be useful in mapping active and fallowed land without having to use field data. Our study accessed a modified FANTA program that includes finer scale Landsat satellite images (Wallace et al., in prep). Note that early forecasts of agricultural extent and productivity can be produced by applying FANTA as soon as the required satellite images are available through GEE. This approach showed that agricultural fallowing dynamics can be captured based on the knowledge of crop spatiotemporal greenness anomalies. The models including months that capture a part of the growing season were effective in capturing fallowing dynamics. The Landsat-based FANTA maps produced in GEE (and including MODIS NDVI to fill no-data values) had high overall accuracy that are comparable to other studies. FANTA captures annual row crops with higher accuracies than perennials (Wallace et al., 2016), making it particularly suited for mapping irrigated crops in the Lower Colorado Basin, which are dominated by annually planted and harvested crops such as cotton, lettuce and broccoli. Additionally, the croplands in the United Stated are mostly annuals which makes FANTA widely applicable.

I conducted the first assessment on agricultural fallowing dynamics in relation to climate and management within the lower Colorado River Basin from 2001 to 2017. Our maps showed differences in spatiotemporal dynamics of irrigated crop extent within the different areas by inter-annual variability and overall extent. Due to the high demand of crops from LCRP, provides 90% of leafy vegetables in the United States, inter-annual variability remained low while overall extent remained high. Conversely, AMA had high inter-annual variability and lower overall extent. The correlation analysis revealed that meteorological indicators correlate with extent variabilities and NDVI. In a semi-arid region, even highly irrigated fields, correlations between climate and irrigated active crop NDVI is revealed (Figure 7). These correlations vary in regards of the best correlated climate variable with NDVI in LCRP area

(average temperature) and AMA (precipitation). Results were to be expected, as agriculture within the LCRP area have low dependency or precipitation due to high levels of irrigation water demand (1.85 afy/30m2 2001-2005) and very low average rainfall (≤ 5 inch) and more dependency on temperature. AMA irrigated agriculture have high dependency on precipitation due to lower irrigation demand (0.73 afy/30m2 2001-2005) and higher precipitation rates (≤ 10 inch). Furthermore, row crops are the first to be impacted by climate through intentional fallowing in response to drought (Gianelli 2015).

Market value, or the prices received by producers for their commodities, also has an influence on irrigation dynamics. Market value influences were examined for high and low agricultural demand years. The results show that the relationship between climate to irrigation extent and NDVI becomes decoupled as the value of crops decrease for PAMA (Figure 8). In contrast, when demand is high, irrigation extent and iNDVI has a higher correlation to climate predictors. This suggests that farmers were making decision on how much area to plant based on climate during high market-value years. Additionally, iNDVI values increase and are tightly coupled with climate when market value is high. This suggests that favourable climate conditions increase incentives to enhance crop greenness through management inputs such as irrigation and fertilizers. The influence of market value and climate can be clearly seen in the PAMA region of interest, while LCRP displayed consistently high NDVI values and stable active extent (Figure 8). This suggests that water rights and access to water influence these relationships. Although, beyond the framework of this study, differences between close proximity irrigation districts with variations in water rights, water sources, policy and management decisions can influence agricultural dynamics. These can include decisions for choosing crop type, irrigation method and irrigation depth.

5. CONCLUSION

The main objective of this research was to assess the dynamics of agricultural fallowing and crop productivity within the Lower Colorado River Basin. I found that LCRP varied very little in agricultural extent from year to year (87-90% active) compared to PMAMA (77-84% active). Agricultural extent and productivity in both regions was found to be sensitive to biophysical factors, with LCRP most sensitive to aridity (R^2=0.369) and PMAMA most sensitive to precipitation (R^2=0.351). These results document that water rights status, which determines and prioritizes access to water, is the dominant factor influencing cropland dynamics. Producers in the LCRP with senior water rights are buffered from climate and market value volatility (relative to those in PMAMA with junior water rights) as revealed in more stable active crop extents and decoupling of productivity from precipitation. Finally, I found market value increased sensitivity to climate, such that agricultural productivity was highest when both biophysical constraints were low and market values were high. The framework developed here utilizes simple freely available, near real-time data inputs to produce information of high value to regional land managers and policy makers. The framework enables the separation of fundamental land management decisions included the decision to crop and/or allocate resources to a given land parcel. The separation of these key factors further enables the exploration of their correlation to biophysical factors such as drought and socioeconomic factors such as the value of the crop. Additionally, the approach developed here is transferable to other regions by simply updating the FANTA model input data and tuning a few key parameters related to average growing season timing.

AWKNOWLEDGMENTS

I would like to thank my graduate advisor Dr. William Kolby Smith for guiding me throughout the graduate program. My sincere gratitude to committee members Dr. Cynthia Wallace and Dr. Wim van Leeuwen who warmly accepted to be on my committee and provided me with insightful suggestions and guidance. I would like to thank Dr. Matthew Dannenberg, Dr. Dong Yan, Jesus Rodriguez, Nathaniel Paul Robinson, Pratima K C, Xian Wang and Amy Hudson for helping me throughout different stages of this research and providing fundamental support for a successful research study. Finally, I would like to thank my family and friends for their advice, support, guidance, encouragement, and the patience throughout my graduate career.

REFERENCES

Anderson, J. R. (1976). A land use and land cover classification system for use with remote sensor data (Vol. 964). US Government Printing Office.

Bastiaanssen, W. G., Molden, D. J., & Makin, I. W. (2000). Remote sensing for irrigated agriculture: examples from research and possible applications. Agricultural water management, 46(2), 137-155.

Bontkes, T. S., & van Keulen, H. (2003). Modelling the dynamics of agricultural development at farm and regional level. Agricultural Systems, 76(1), 379-396.

California Department of Food and Agriculture. California Agricultural Statistics Review 2014–2015. Available online: https://www.cdfa.ca.gov/statistics/PDFs/2015Report.pdf (accessed on 10 July 2018).

Challinor, A.J.; Watson, J.; Lobell, D.B.; Howden, S.M.; Smith, D.R.; Chhetri, N. A meta-analysis of crop yield under climate change and adaptation. Nat. Clim. Chang. 2014, 4, 287–291.

Chen, Y., Lu, D., Luo, L., Pokhrel, Y., Deb, K., Huang, J., & Ran, Y. (2018). Detecting irrigation extent, frequency, and timing in a heterogeneous arid agricultural region using MODIS time series, Landsat imagery, and ancillary data. Remote Sensing of Environment, 204, 197-211.

Cohen, M. J., Martin, J. C., Ross, N., & Luu, P. (2011). Municipal Deliveries of Colorado River Basin Water. Pacific Institute, Berkeley, California, USA.

Deines, J. M., Kendall, A. D., & Hyndman, D. W. (2017). Annual irrigation dynamics in the US northern high plains derived from Landsat satellite data. Geophysical Research Letters, 44(18), 9350-9360.

Fan C., Zheng B., Myint S. W., & Aggarwal R. (2014). Characterizing changes in cropping patterns using sequential Landsat imagery: an adaptive threshold approach and application to PMAMA, Arizona. International Journal of Remote Sensing, 34(20), 7263-7278.

Galletti, C. S., & Myint, S. W. (2014). Land-use mapping in a mixed urban-agricultural arid landscape using object-based image analysis: A case study from Maricopa, Arizona. Remote Sensing, 6(7), 6089-6110.

Galvão, L. S., Epiphanio, J. C. N., Breunig, F. M., & Formaggio, A. R. (2018). 6 Crop Type Discrimination Using Hyperspectral Data. Biophysical and Biochemical Characterization and Plant Species Studies, 183.

Gianelli, W. R. 2015. Water Leaders 2015 Class Report: Managing Drought for the Economy and the Environment. Sacramento, CA: Water Education Foundation. http://www.watereducation.org/post/2015-class-report.

Huckleberry, J. K., & Potts, M. D. (2019). Constraints to implementing the food-energy-water nexus concept: Governance in the Lower Colorado River Basin. Environmental Science & Policy, 92, 289-298.

Nuckols, J.R.; Gunier, R.B.; Riggs, P.; Miller, R.; Reynolds, P.; Ward, M.H. Linkage of the California Pesticide Use Reporting Database with spatial land use data for exposure assessment. Environ. Health Perspect. 2007, 115, 684.

Pulwarty, R. S., Jacobs, K. L., & Dole, R. M. (2005). The hardest working river: drought and critical water problems in the Colorado River Basin. Drought and water crises: Science, technology, and management issues, 249-285.

Shivers, S., Roberts, D., McFadden, J., & Tague, C. (2018). Using Imaging Spectrometry to Study Changes in Crop Area in California's Central Valley during Drought. Remote Sensing, 10(10), 1556.

Smith, H. V. (1956). The climate of Arizona. College of Agriculture, University of Arizona (Tucson, AZ).

Wallace, C. S., Thenkabail, P., Rodriguez, J. R., & Brown, M. K. (2017). Fallow-land Algorithm based on Neighborhood and Temporal Anomalies (FANTA) to map planted versus fallowed croplands using MODIS data to assist in drought studies leading to water and food security assessments. GIScience & Remote Sensing, 54(2), 258-282.

Wu, Z., Thenkabail, P. S., Mueller, R., Zakzeski, A., Melton, F., Johnson, L., ... & Verdin, J. P. (2014). Seasonal cultivated and fallow cropland mapping using MODIS-based automated cropland classification algorithm. Journal of Applied Remote Sensing, 8(1), 083685.

APPENDIX B: TABLES

	Warm Season	Cool Season
NDVI (Growing Season-DOY)	97-273	1-97 and 273-365
Precipitation (Month)	5-10	1-5 and 10-12
Average Temperature (Month)	5-10	1-5 and 10-12
VPD (Month)	5-10	1-5 and 10-12
Aridity (PPT/PET) (Month)	5-10	1-5 and 10-12

Table 1. Seasonal divisions of research variables such as NDVI and meteorological data.

	Climate Variable	Precipitation	Average Temperature	VPD	Aridity
PHOENIX NDVI	Season	**Warm**	Warm	**Warm**	**Warm**
	R^2	**0.351**	0.064	**0.387**	**0.369**
	p	**0.007**	0.17	**0.005**	**0.006**
	slope	**765**	-4.4	**-27**	**0.93**
PHOENIX NDVI	Season	Cool	Cool	Cool	Cool
	R^2	-0.048	0.093	-0.03	0.01
	p	0.62	0.13	0.48	0.3
	slope	-230	7.5	0.48	-0.97
YUMA NDVI	Season	**Warm**	Warm	Warm	Warm
	R^2	**0.121**	-0.059	0.124	-0.031
	p	**0.094**	0.75	0.091	0.24
	slope	**389**	1.6	21	0.31
YUMA NDVI	Season	Cool	**Cool**	**Cool**	Cool
	R^2	-0.67	**0.486**	**0.506**	-0.66
	p	0.99	**0.001**	**0.001**	0.93
	slope	-3.1	**20**	**36**	-0.066

	Climate Variable	Precipitation	Average Temperature	VPD	Aridity
PHOENIX EXTENT	Season	Warm	Warm	Warm	Warm
	R^2	-0.0645	0.008	-0.062	-0.057
	p	0.86	0.31	0.81	0.72
	slope	-66	4	3.2	-0.17
PHOENIX EXTENT	Season	Cool	Cool	Cool	**Cool**
	R^2	0.086	-0.042	-0.04	**0.211**
	p	0.13	0.56	0.54	**0.036**
	slope	794	3.5	-4.9	2.2
YUMA EXTENT	Season	Warm	Warm	**Warm**	Warm
	R^2	-0.044	0.033	**0.211**	-0.039
	p	0.58	0.23	**0.036**	0.54
	slope	184	-7.9	**-34**	0.22
YUMA EXTENT	Season	Cool	**Cool**	**Cool**	Cool
	R^2	-0.061	**0.219**	**0.272**	-0.065
	p	0.79	**0.033**	**0.019**	0.86
	slope	146	**-20**	**-38**	0.18

Table 2. Summary statistics shows PMAMA warm season climate variables linear correlation to summer growing season greenness variability and LCRP area cool season

APPENDIX C: FIGURES

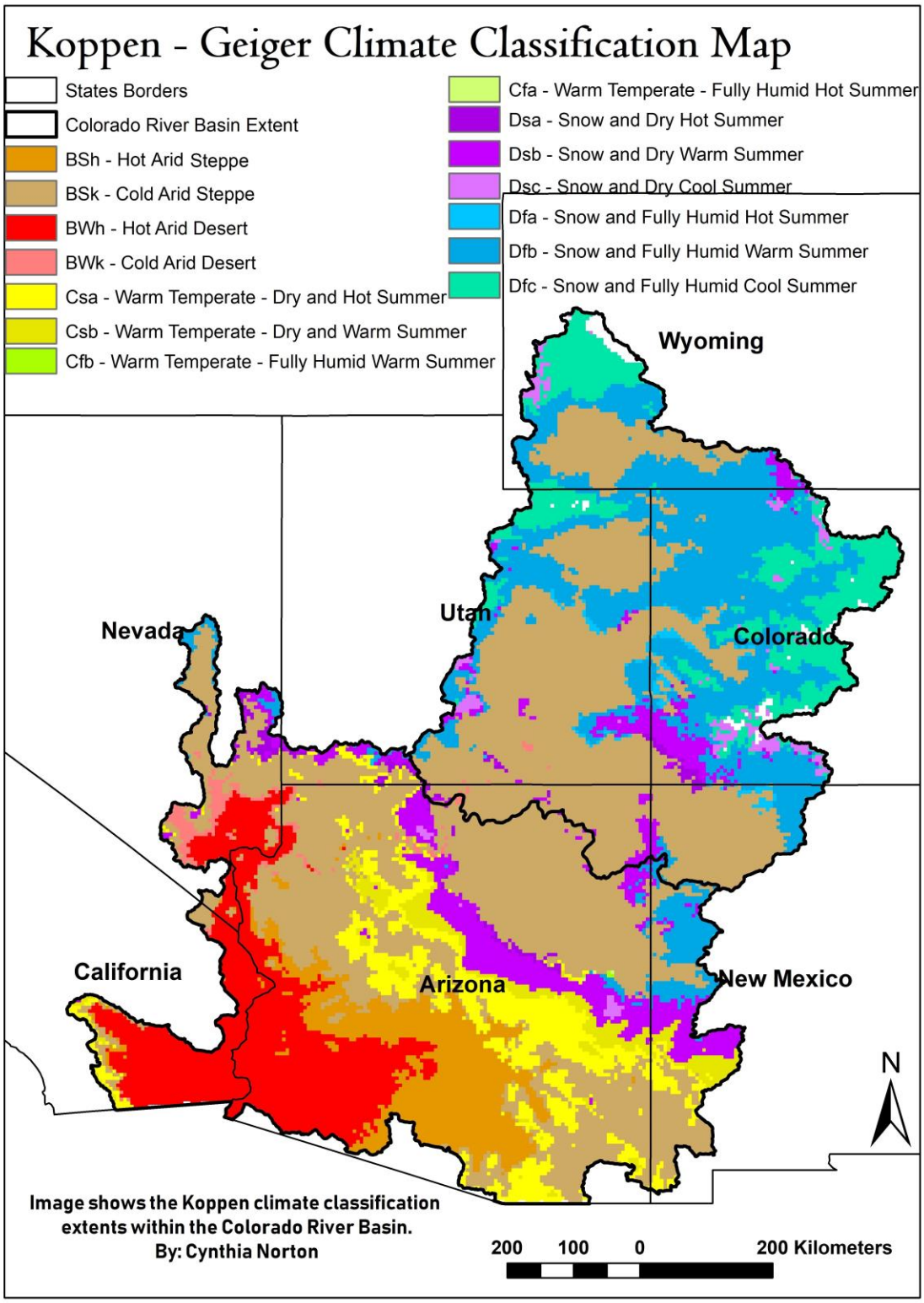

Figure 1: Koppen Climate Classification within the Colorado River Basin. Image shows types of climate within the basin.

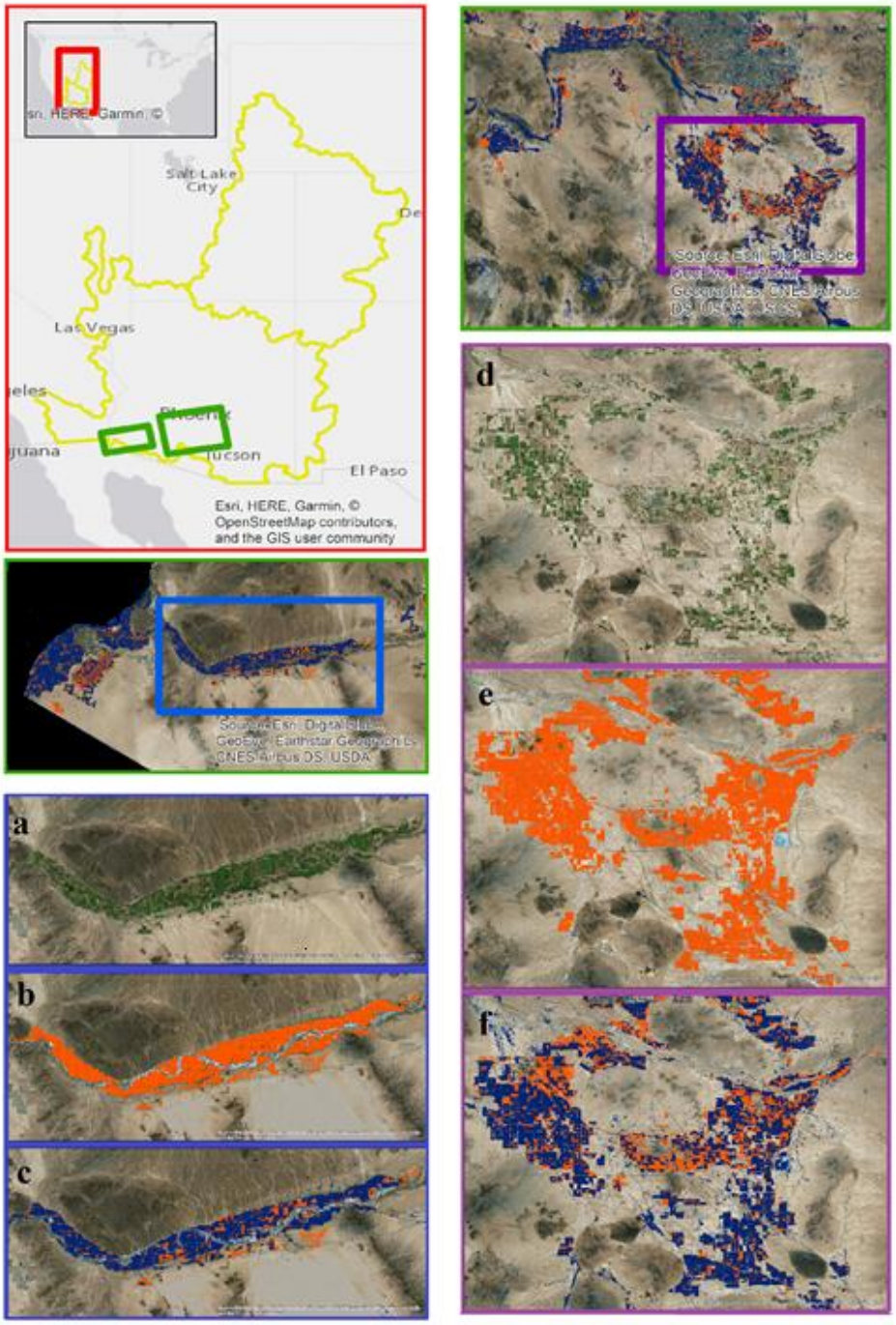

Figure 2. Figure shows an example of the methodology for masking. Masking starts from masking the biophysical signal true color composite (a and d) with the orange colored symbolized NLCD (b and e) and then masking with the FANTA classified map, symbolized with blue. The orange colors peeking out of the blue agriculture active crop extent show areas in fallow during the growing season of the year. a) LCRP County southwest Arizona true color image. b) LCRP County southwest Arizona NLCD overlay. c) LCRP County southwest Arizona FANTA overlay. d) South central PMAMA Arizona area true color image. e) South central PMAMA Arizona area NLCD f) South central PMAMA Arizona area FANTA.

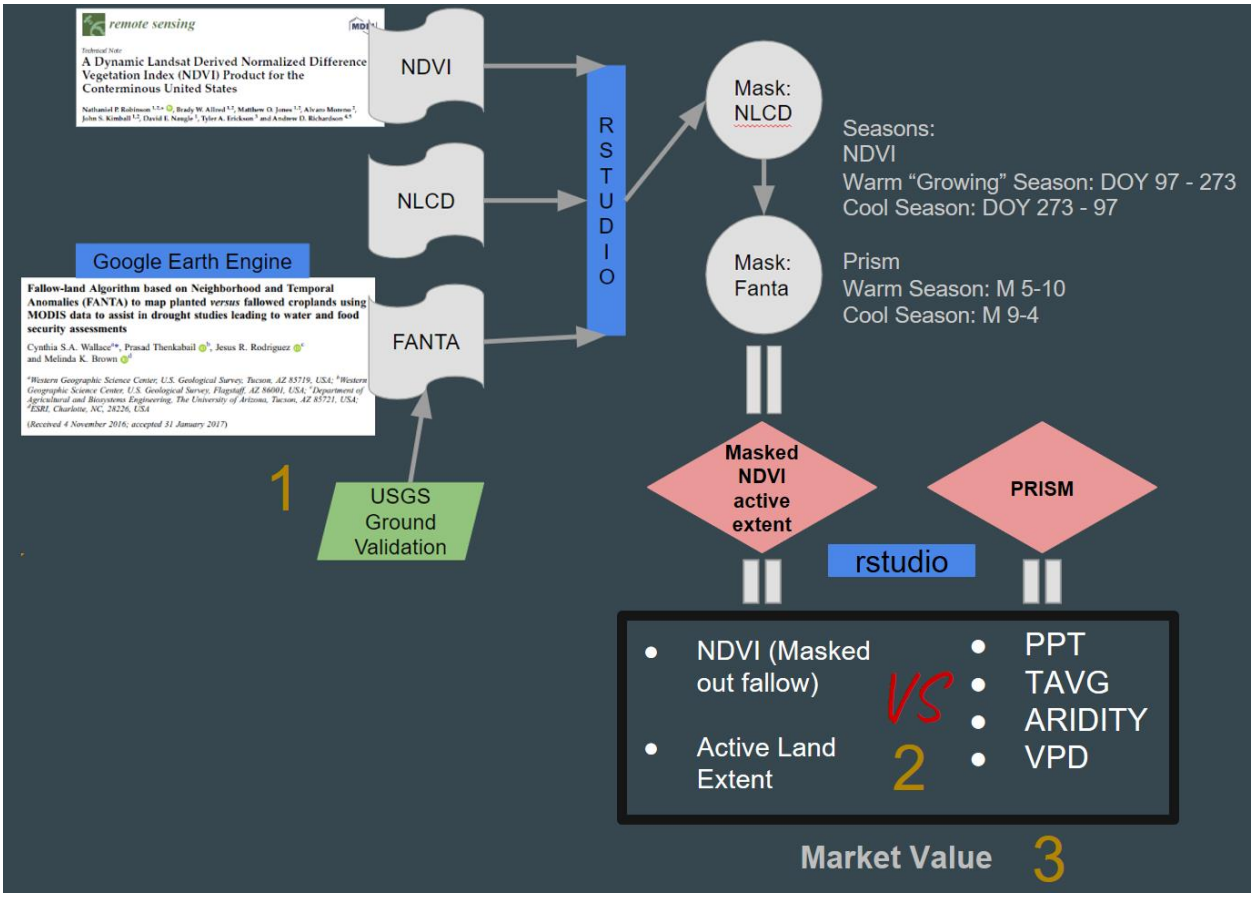

Figure 3. Image shows flow chart of research methodology. The chart shows datasets used for masking active crop biophysical signal. Image shows which parts of the methodology corresponds to specific research question. The FANTA classification step (1) aids in assessing inter-annual trends of agricultural fallowing and active crop extent dynamics. Within the R-studio interface, the NLCD was used to mask agricultural boundaries while FANTA was used to mask active crop and fallow biophysical NDVI signal. This leads to the creating linear models to assess biophysical active crop signal response to climate (2). The third step (3), addresses socioeconomic drivers of NDVI and its influence to the relationship between climate and NDVI.

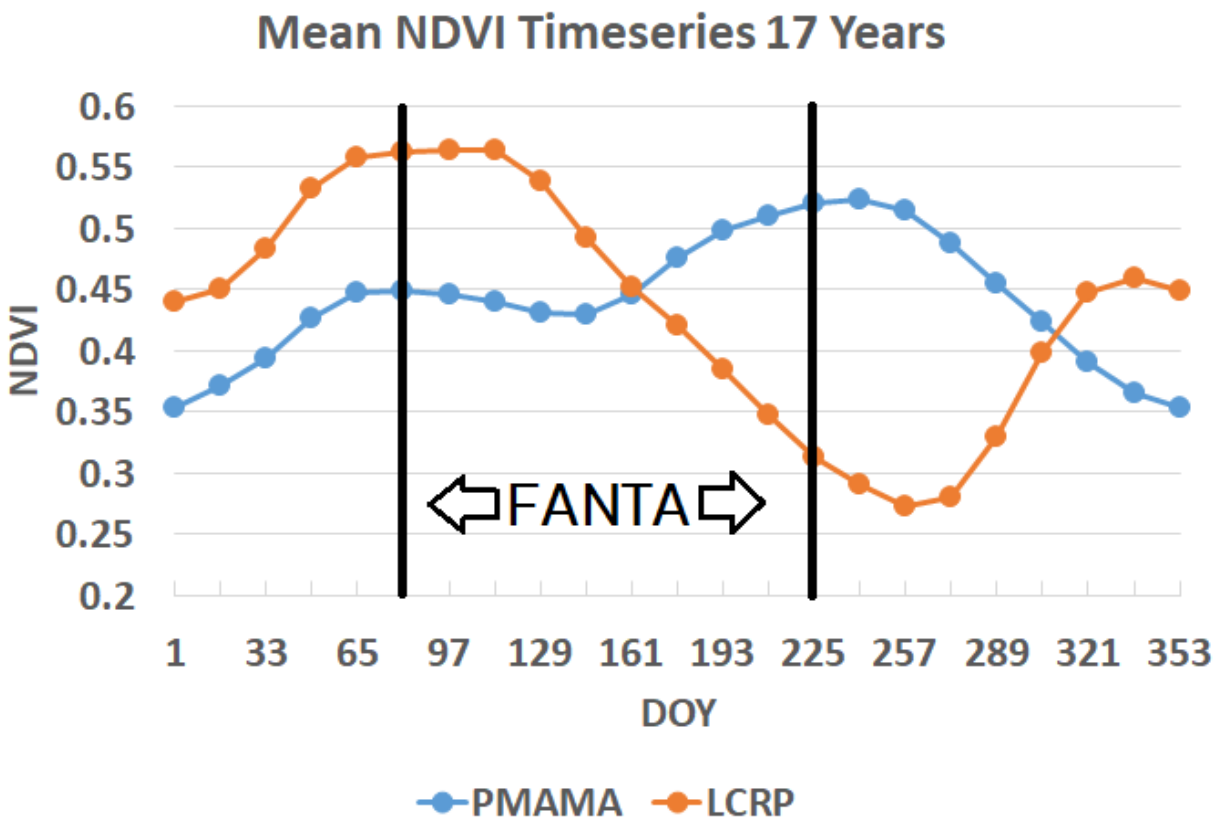

Figure 4: Image shows a mean inter-annual time series of agricultural biophysical signal and the Fanta months (April, May, June, July) used for classification.

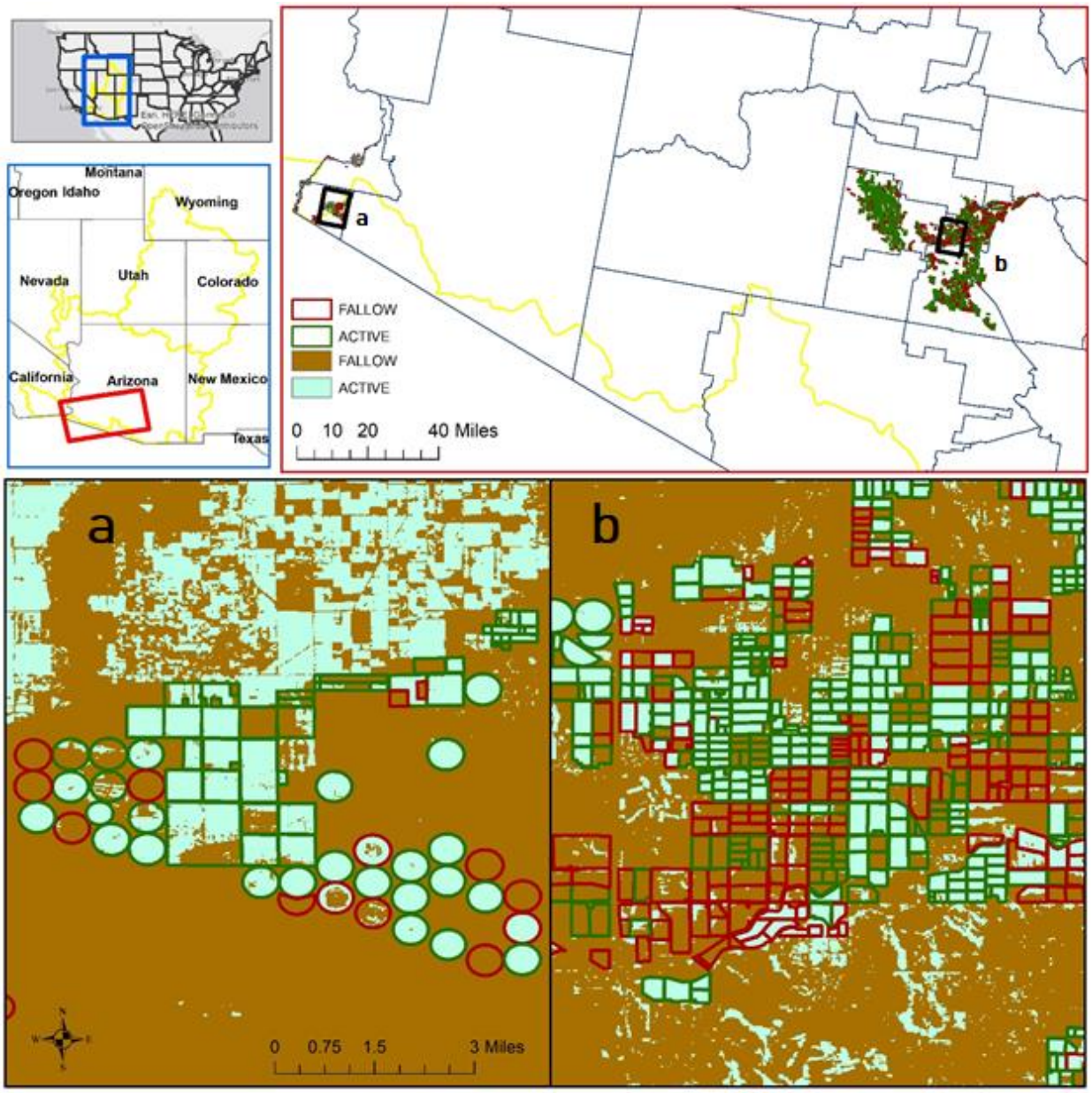

Figure 5. Image shows a visualization of classification accuracy. The outlined polygons represent validation data provided by the USGS while filled colors are from the classified FANTA image. a) LCRP area 2017 ground validation polygons overlaid on FANTA for the year 2017. b) PMAMA area 2014 ground validation polygons overlaid on a 2014 FANTA layer. If the green outline is overlaid over the green classification, this resulted in an accurately classified active plot while green outline over fallow classification symbolized as brown results in an incorrectly classified plots. Red outline over brown overlaid FANTA results in an accurately classified fallow plot while red outline over green overlaid means it was a fallow plot classified as active.

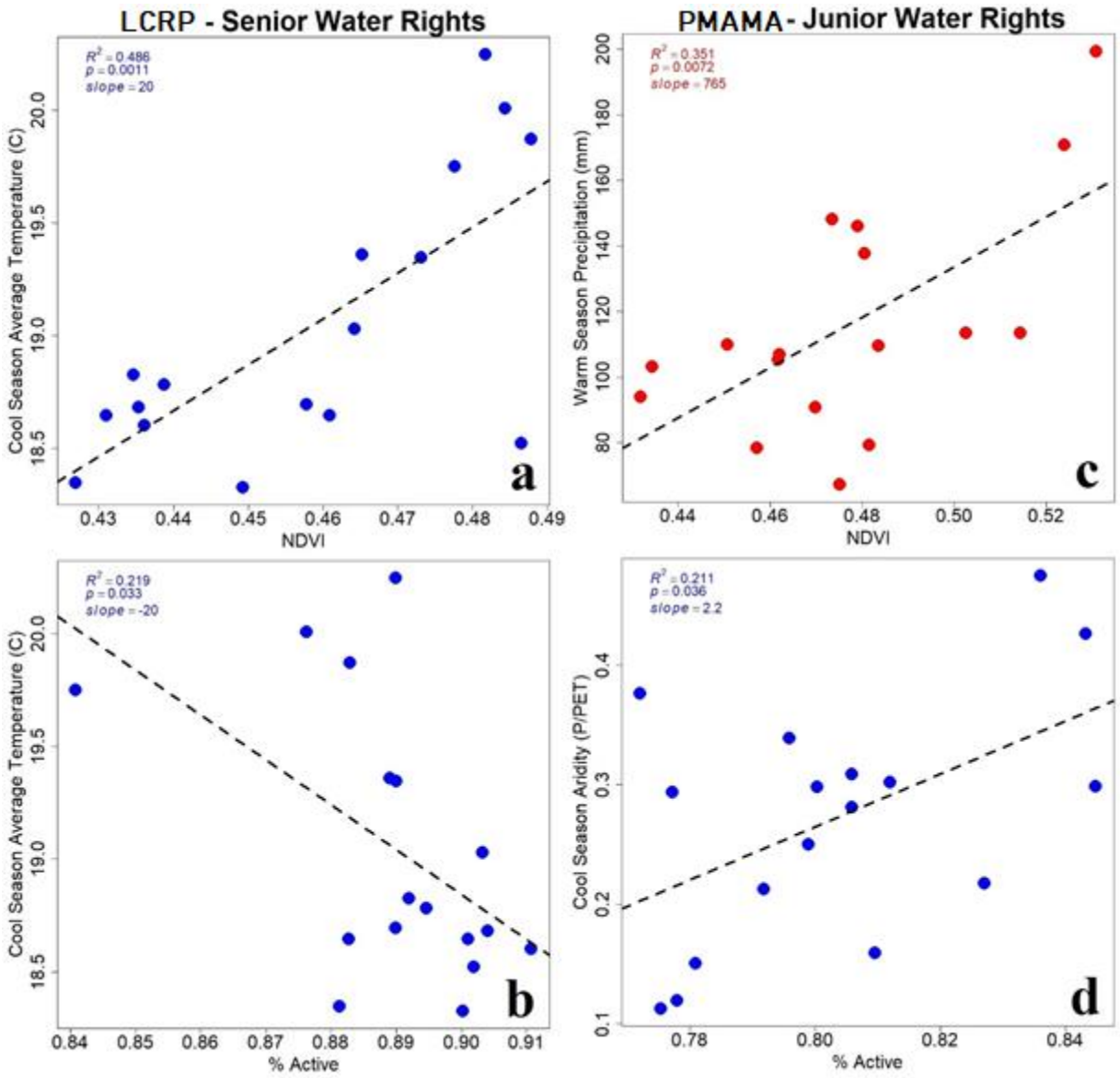

Figure 6. Significant linear regressions on irrigated area over time, crop NDVI and associated drivers. a) LCRP area linear regression of mean winter growing season NDVI versus cool season temperature. b) LCRP area linear regression of percent irrigated active crop versus yearly mean temperature. c) PMAMA area linear regression of mean summer growing season NDVI versus warm season precipitation d) PMAMA area linear regression of percent irrigated active crop versus cool season aridity (P/PET). LCRP region showed biophysical response signal NDVI and extent sensitivity to dominant climate predictor cool season average temperature. PMAMA biophysical signal and extent show sensitivity to precipitation and cool season aridity.

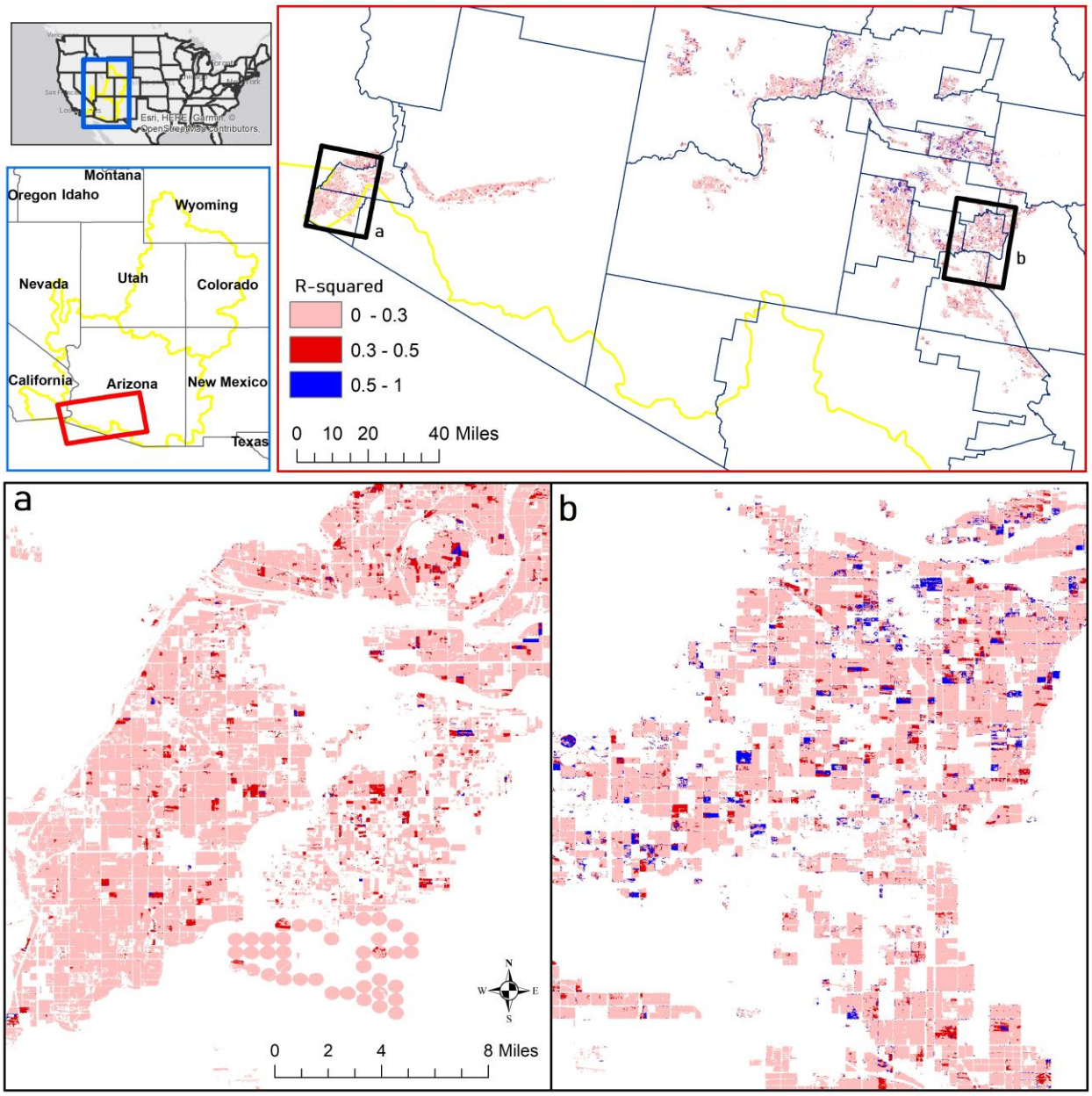

Figure 7. Spatial explicit correlations between NDVI and FANTA versus climate variable. a) LCRP area spatial explicit relationship of mean winter growing season NDVI versus cool season temperature b) LCRP area spatial explicit relationship of percent irrigated active crop versus cool season temperature. Despite differences in water rights, both regions correlate to dominant regional climate predictor.

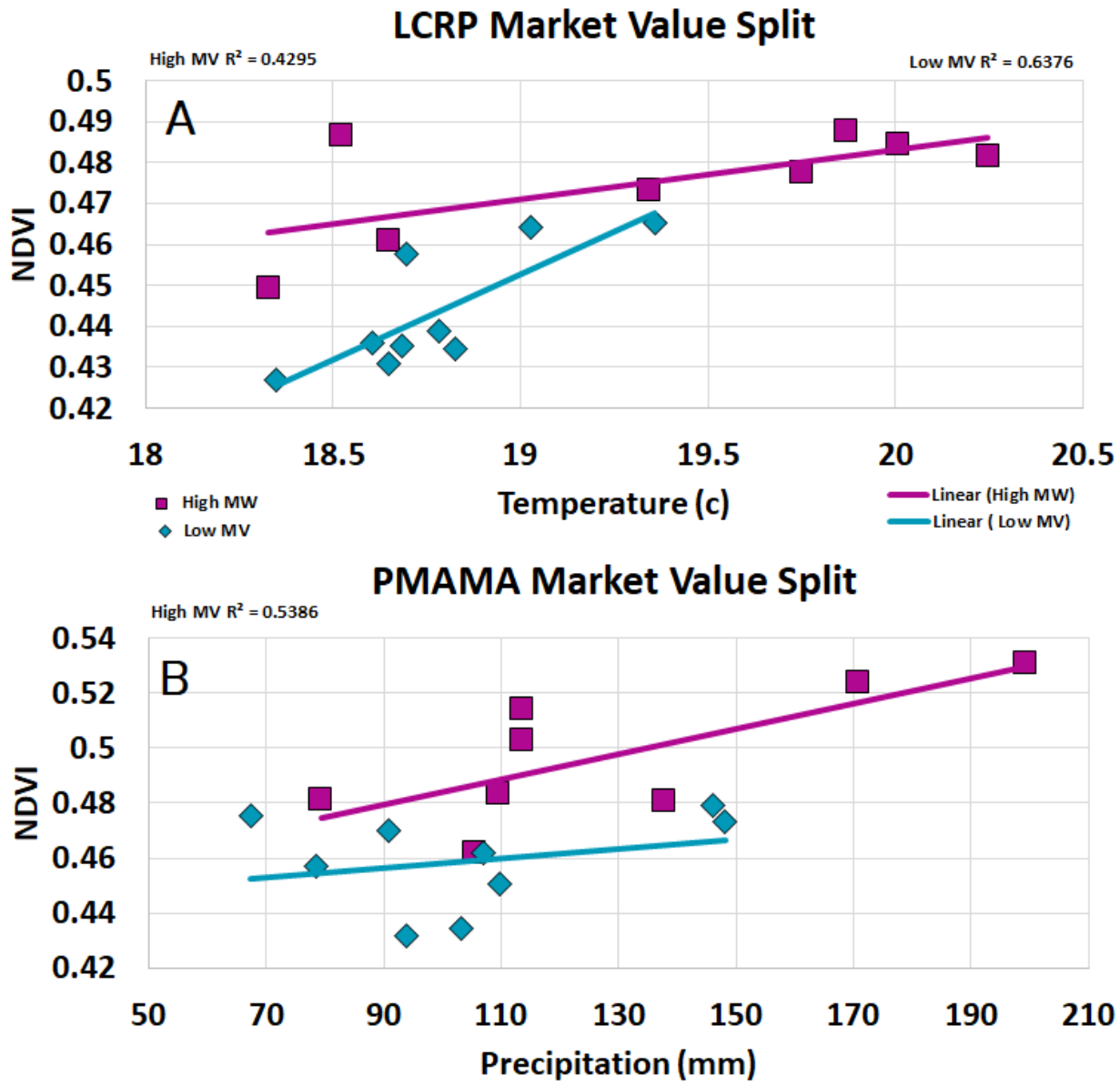

Figure 8. Trends in NDVI versus climate variable for years with a split of high and low market value years. a) LCRP area linear regression of mean winter growing season NDVI versus cool season temperature with a market value split. b) PMAMA area linear regression of mean summer growing season NDVI versus warm season precipitation with a market value split. Both regions show higher biophysical signal values on high market value years compared to low market value years. This suggests a change in management practice to maximize crop productivity.

APPENDIX D: SUPPLEMENTAL FIGURES

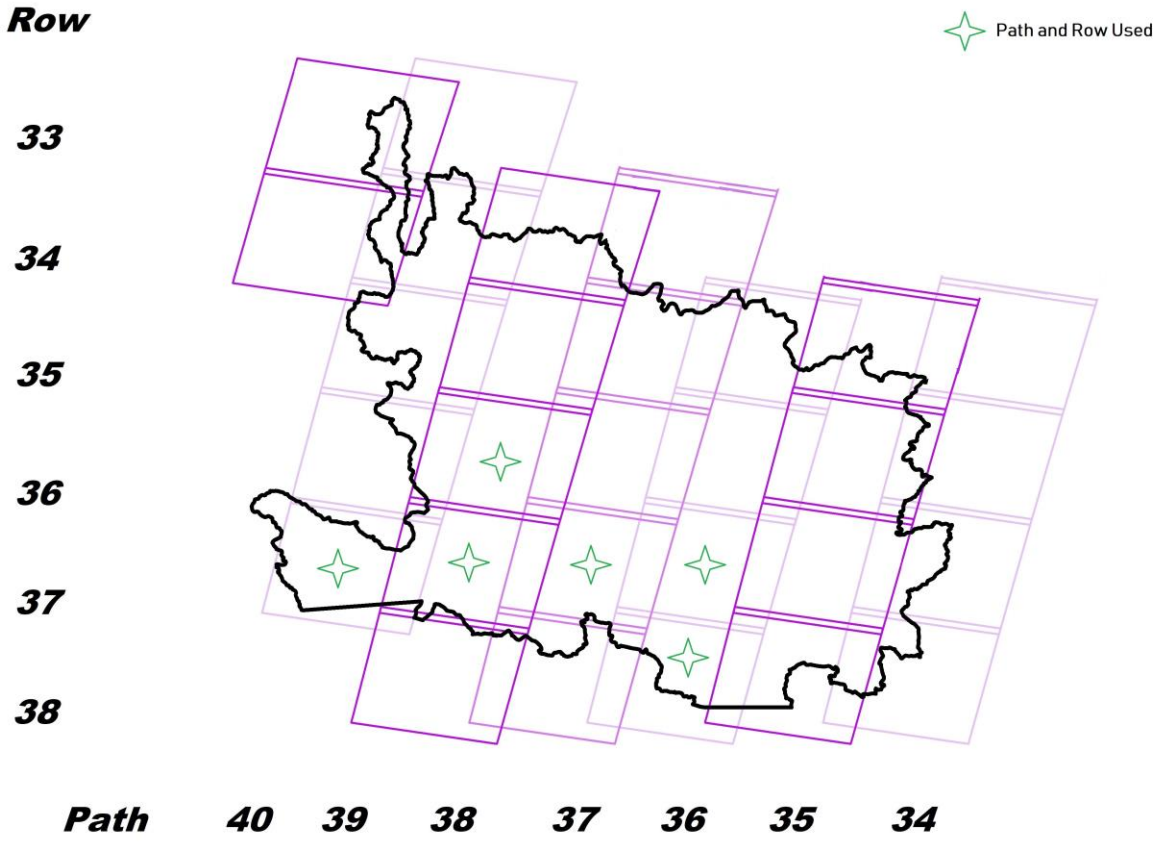

Figure 1. Figure shows scenes path row outline overlaid on the lower Colorado Basin. Green stars show exact scene path rows chosen for regions of interest within the lower Colorado Basin.

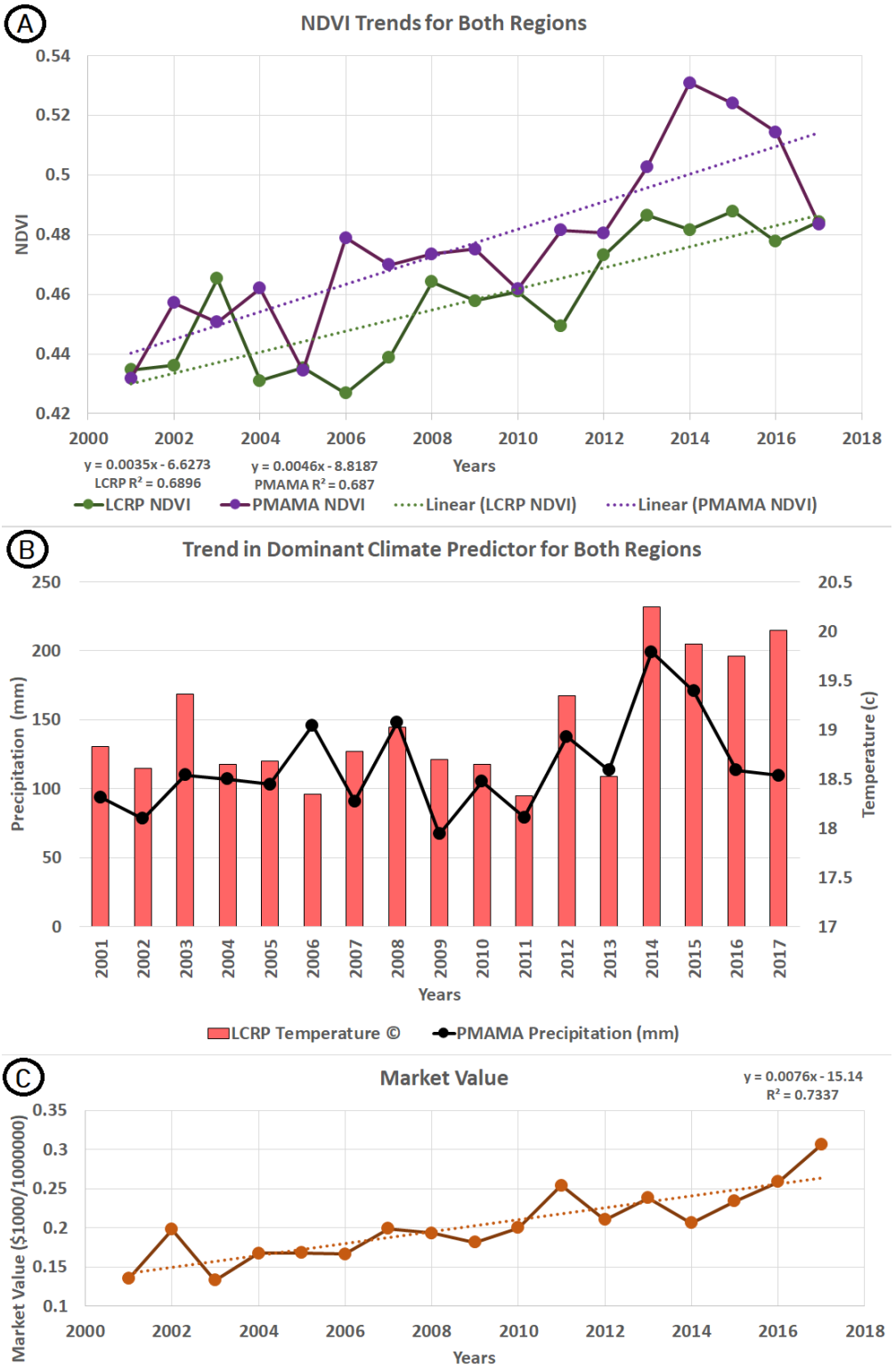

Figure 2. Regional climate and biophysical trends within study area. a) Biophysical greenness NDVI trends for both LCRP and PMAMA b) LCRP mean growing season temperature (b) trends for all 17 years and PMAMA overall growing season precipitation trends for all 17 years. c) Market value of agricultural crop production sold trends using Arizona agricultural statistics.

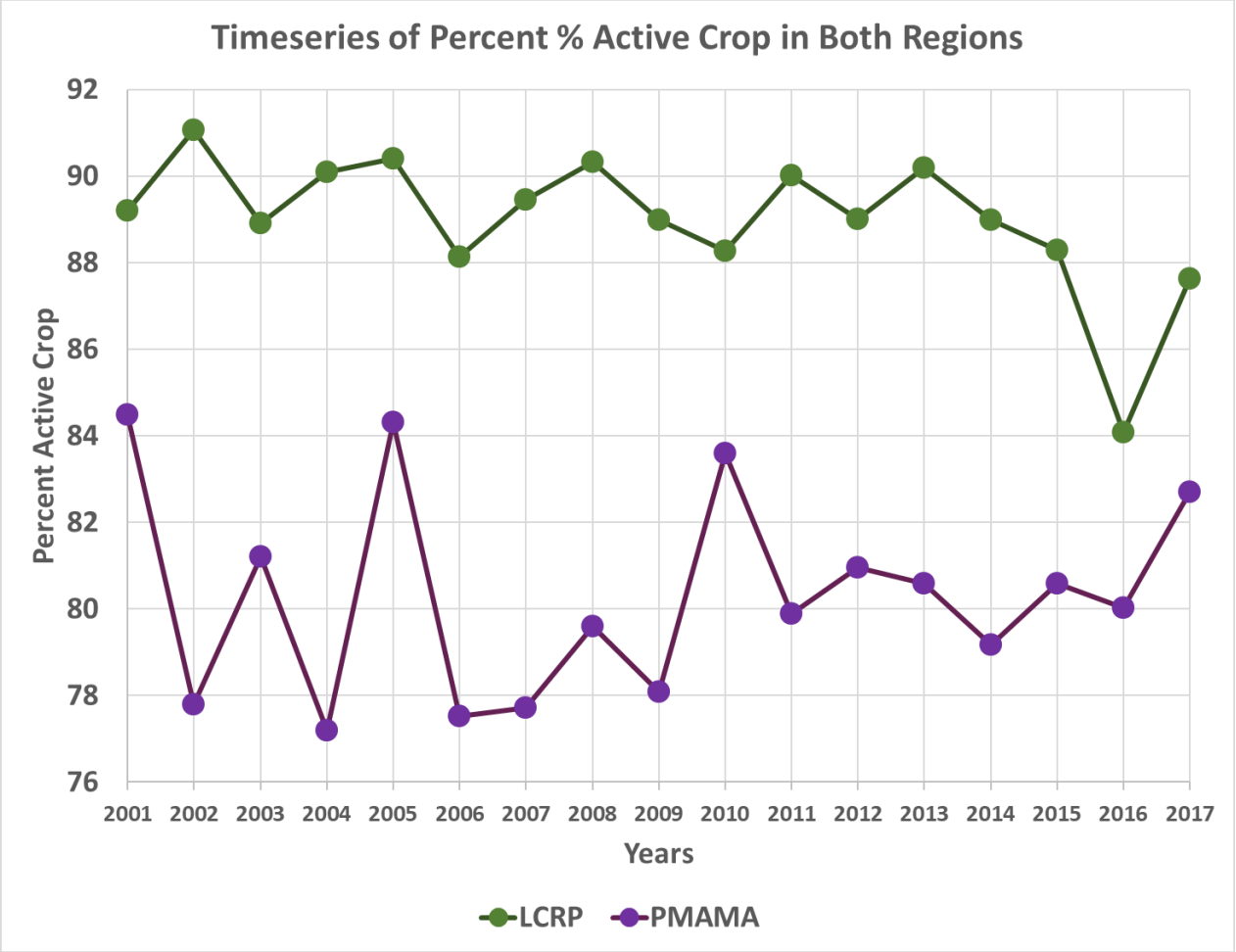

Figure 3. Integrated fallowing trends for both LCRP and PMAMA regions. Image shows percent area with active crop for all 17 years. Plot shows LCRP region having overall active crop extent higher throughout all the years compared to PMAMA. Additionally, LCRP show less inter-annual variability in crop extent compared to PMAMA.

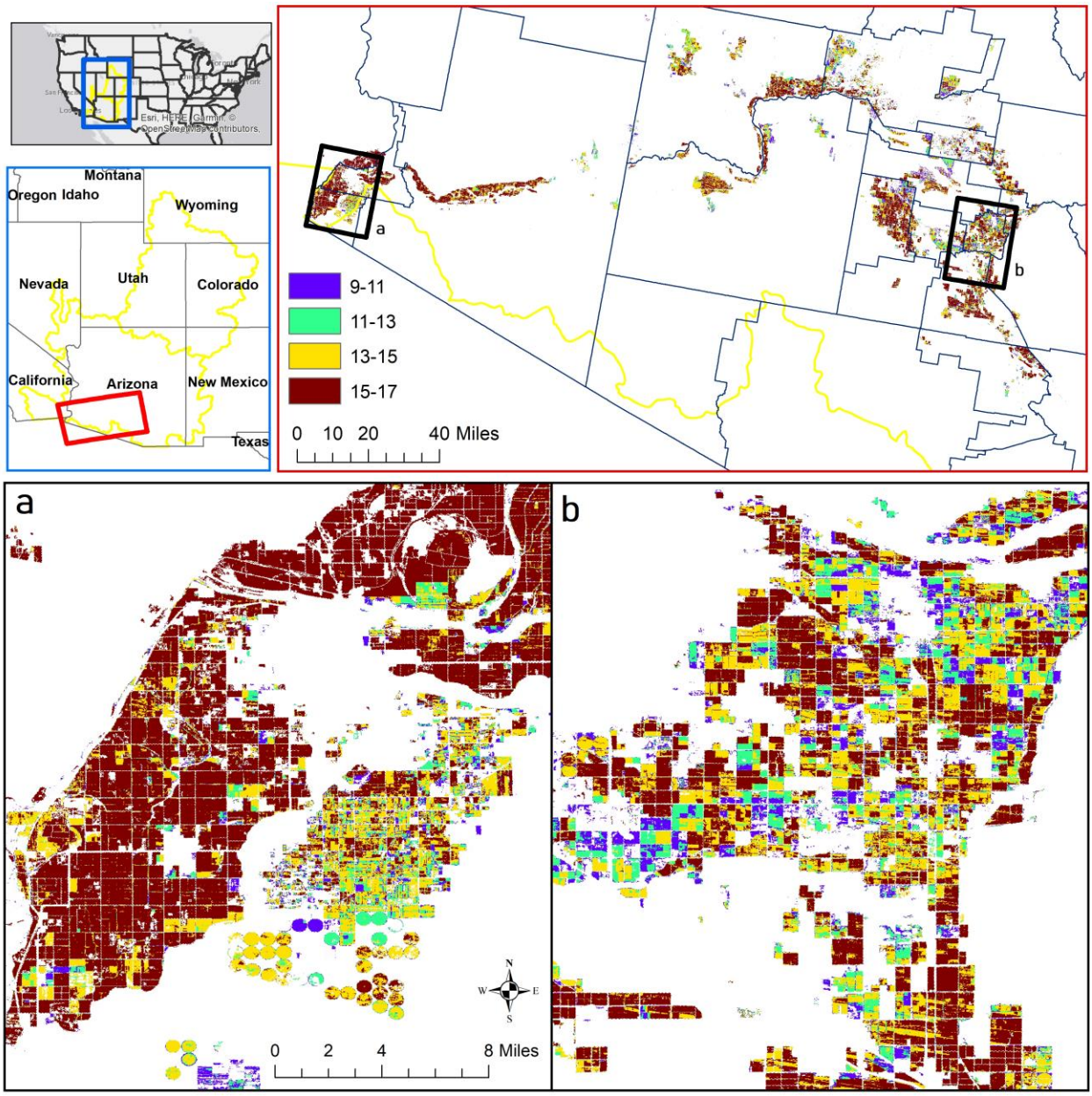

Figure 4. Spatial explicit fallowing trends within both regions. Additionally, figure shows how many pixel data layers were used for spatial explicit correlations of biophysical NDVI values with climate. The brown pixels represent 15-17 years of active crop (1-2 years of fallowing) occurred in the pixel's footprint and the change in colors, fallowing years = yellow (2-4 years), green (4-6 years) and purple (6-8 years), represent additional years of fallowing has occurred. a) LCRP region spatial explicit fallowing dynamics. b) PMAMA region spatial explicit fallowing dynamics. LCRP region has less inter-annul variability in fallowing dynamics compared to PMAMA.

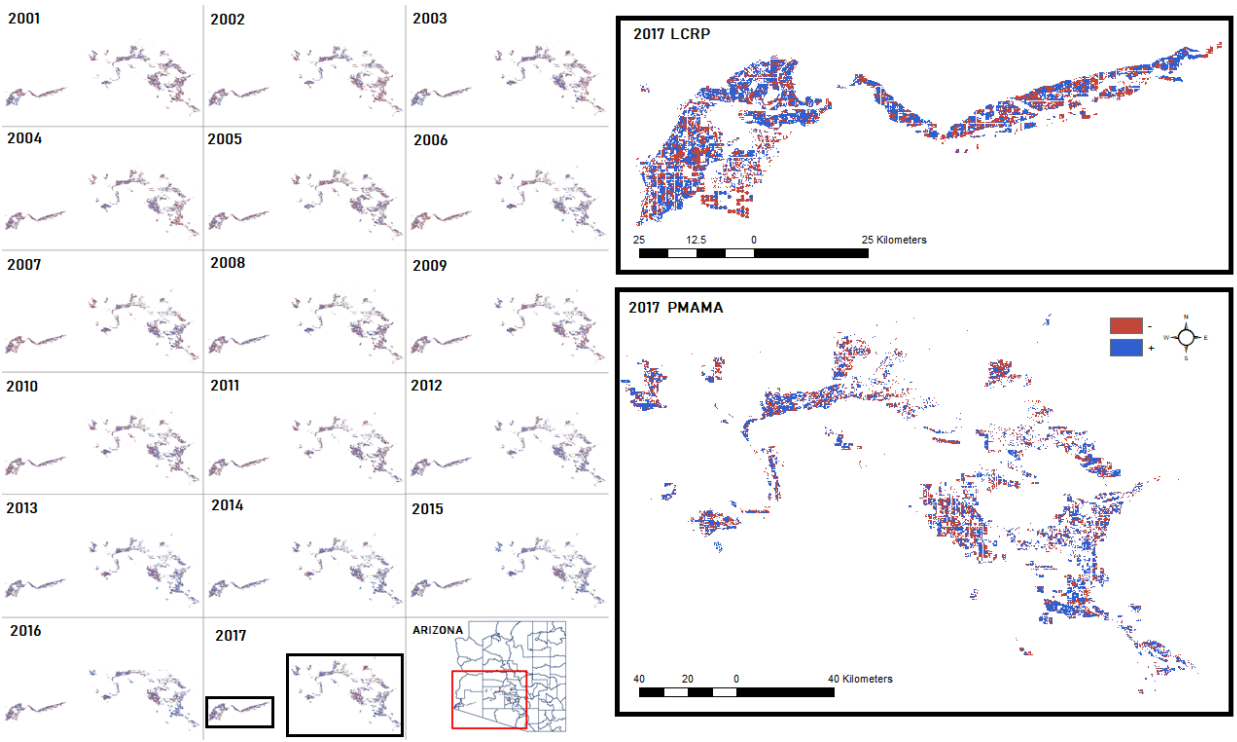

Figure 5: NDVI anomalies for both regions for all 17 years. Each scene shows positive or negative anomalies for both regions. The zoomed insets show spatial explicit anomalies for LCRP and PMAMA for the year 2017. The blue colors represent a positive anomaly (higher NDVI values compared to historical mean) and the red colors are negative anomalies (lower NDVI values compared to historical mean).

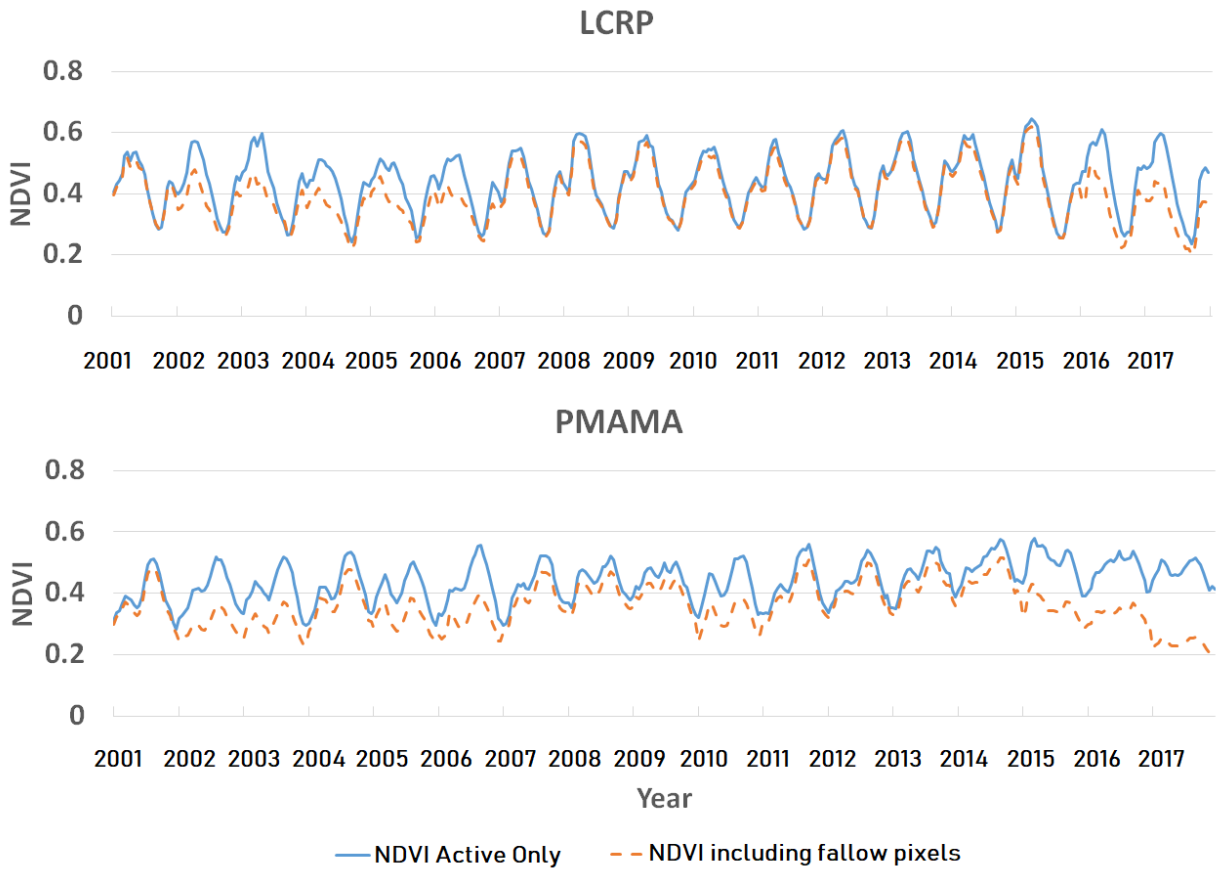

Figure 6: Image shows mean trends in biophysical greenness values when calculated including fallowed pixels (orange) and values without fallowed pixels (blue). The biophysical signal of crops decreased when fallowed pixels are used for calculating integrated greenness NDVI values of active crop.